WELL PLACEMENT OPTIMIZATION AND HISTORY MATCHING USING HYBRID METHODS

A Dissertation

by

JEONG MIN KIM

Submitted to the Office of Graduate and Professional Studies of
Texas A&M University
in partial fulfillment of the requirements for the degree of

DOCTOR OF PHILOSOPHY

Chair of Committee,	Akhil Datta-Gupta
Committee Members,	Michael J. King
	Eduardo Gildin
	Yuefeng Sun
Head of Department,	A. Daniel Hill

August 2015

Major Subject: Petroleum Engineering

ABSTRACT

For field development, hydrocarbon recovery is considered as one of the main objectives through the whole life cycle of the field. The reservoir management during the field development ranges from planning for the field development, drilling and well optimization and rejuvenation of the mature field till abandonment. The ultimate goal of field development comes down to maximizing profits. Better understanding of the reservoir is essential to achieve this goal. Among the many problems of reservoir management, well location optimization for maximum recovery and prediction of the reservoir performance are important ones to solve.

We propose a hybrid sampling method for the well placement problem. To decide on the well location, evolutionary algorithms were used and updated starting from an initial response surface consisting of the candidate well locations selected using random sampling method as well as a dynamic measure probability map serving as an indicator of remaining hydrocarbon in the reservoir. We applied this approach to a mature field case because the dynamic measure can capture the complex response of the reservoir and provide information of sweep and drainage areas.

We presented a well placement optimization method for primary depletion in green fields. Unlike the complex responses in the mature field, pressure depletion is the main recovery mechanism in the green field. For pressure depletion in green fields, we adopted diffusive time of flight, instead of convective time of flight for the dynamic measure. By using a fast marching method, we can get the propagation of the pressure

front very fast with a single non-iterative calculation. This diffusive time of flight was consolidated into the dynamic measure probability map which is the starting point of our search space, for the evolutionary algorithm. This method was extended to a dual porosity model by considering the flow between matrix and fracture.

Finally, a structured history matching approach which consists of global calibration and local calibration is presented. Key global parameters which heavily affect the model response are selected through a sensitivity analysis. Design of experiments and response surface methodology with evolutionary algorithms such as genetic algorithm are used to calibrate these key global parameters. Then, local calibration using streamline based sensitivity and generalized travel time inversion technique is performed.

DEDICATION

To my family for their unconditional love and support.

ACKNOWLEDGEMENTS

First of all, I express my sincere gratitude to my academic advisor, Dr. Akhil Datta-Gupta, for his guidance, for encouragement and financial support. Without his continuous and generous support, I would haven't completed my doctoral program.

I would like to extend my gratitude to Dr. Michael King, who provided me with valuable insights and encouragement.

I thank my committee members, Dr. Eduardo Gildin and Dr. Yuefeng Sun, for their guidance and support for this research.

Thanks also go to the students and alumni of MCERI and faculty and staff of Petroleum Engineering department for making my time at Texas A&M University a great experience.

NOMENCLATURE

DM	Dynamic Measure
DM_FMM	Dynamic Measure using Fast Marching Method
DTOF	Diffusive Time of Flight
DM_DP	Dynamic Measure for Dual Porosity Model
DV	Drainage Volume
FMM	Fast Marching Method
GA	Genetic Algorithm
GTTI	Generalized Travel Time Inversion
k	Permeability, md
k_{ro}	Oil relative permeability
PV	Pore Volume
S_o	Oil saturation
TTOF	Total Time of Flight

TABLE OF CONTENTS

Page

LIST OF FIGURES

Page

LIST OF TABLES

Page

CHAPTER I

INTRODUCTION

During the field development, hydrocarbon recovery is considered as one of the main objectives for the whole life cycle of the field. The reservoir management during the field development ranges from planning for the field development, drilling and well optimization and rejuvenation of the mature filed through abandonment. The ultimate goal of the field development comes down to maximizing profits. Better understanding of the reservoir is quite essential to achieve this goal. Among the many problems of reservoir management, well location optimization for maximum recovery and prediction of the reservoir are important problems to solve.

1.1 Overview

Finding optimal well locations is one of the significant features of the field development problems. In mature field, it is more complex to locate infill well drilling locations since there are many existing wells in addition to the heterogeneities in the reservoir. It is necessary to capture how the reservoir behaves to find optimal locations but it is harder to catch it in mature field. Well placement problems to be solved are expressed as optimization problems. Well placement optimization could be a problem of maximizing either oil recovery or asset value of the project. In general, the optimization problem of well placement is computationally expensive and it is required to deal with geologic uncertainty.

The optimization methods on well placement problems are traditionally categorized into deterministic and stochastic methods. However, in order to take the advantage of each algorithm, hybrid methods were implemented. Hybrid methods are generally more efficient to find optimal solution. Guyaguler et al. (2002) showed hybrid stochastic algorithms with proxy modelling generally converge to reasonable solution with fewer evaluations compared to stochastic algorithms. The better proxy model that hybrid methods are combined with, the more efficiently the algorithms can find optimal solution.

Dynamic measure proposed by Taware et al. (2012) is the combination of static properties and dynamic properties including Total Time of Flight (TTOF) of streamlines, which are considered as the properties regarding remaining oil in the reservoir. It is a good indicator of where oil remains in the reservoir and provides a possible new well location. However, the point with the highest dynamic measure value is not necessarily the optimal location for additional well. Nevertheless, the point with maximum value of dynamic measure can be expected to be close to the optimal well location and can be used as the starting point for search algorithms. In other words, this dynamic measure can be the source of proxy model for stochastic algorithms.

In the streamline method, the use of the convective time of flight as a spatial variable along streamlines effectively reduces the calculation to only one dimension. For pressure depletion and associated reservoir processes, we expect that the use of the diffusive time of flight will allow similar advancements in methods and applications. The depth of investigation is defined as the propagation distance of peak pressure

disturbance. By using asymptotic expansion of the diffusivity equation, the propagation of the pressure front for heterogeneous reservoirs, which is in the form of Eikonal equation, is obtained. By solving this equation with Fast Marching Method, a diffusive time of flight at each and every cell within the domain is calculated. The advantage of using Fast Marching method lies in that frontal propagation is obtained very fast with a single non-iterative calculation. For primary depletion field, diffusivity time of flight term from fast marching method can be a component of dynamic measure in place of convective time of flight from streamlines.

To understand the proper geologic characteristics in the reservoir is one of the key aspects of reservoir management. However, in the field with the geological complexity, the reservoir characterization can be quite challenging because the reservoir fluid dynamics are a composite response of the heterogeneous geologic feature and the field operations. Most of deterministic approaches generally start with a single initial geological model so that they strongly depend on quality of the initial model. There have been many cases of misrepresentation of large-scale features such as fault communications and pore volumes resulting in unphysical model updates in fine scale reservoir permeability. This is due to the local search nature of the deterministic technique and its deficiency in handling various scale uncertainties.

Global search algorithms avoid the problem of convergence to local optimum nearest to the initial starting and are able to reconcile multi-scale uncertainties simultaneously. Global search techniques have been known to be effective for history matching problems. The advantage of these stochastic search techniques is that they

require neither complicated differential equations nor a smooth response space. The primary challenge is that they require large number of flow simulations, which can be computationally prohibitive when the parameter space is very large. Consequently, sensitivity analysis is introduced to rank the importance of model parameters and screen insignificant ones, and the proxy model is introduced as a surrogate to avoid simulations for less likely model candidates (Cheng et al. 2008; Yeten et al. 2005).

1.2 Outline of Dissertation

In Chapter II, we will present a hybrid sampling method which obtain a proxy model built by initial candidate well locations sampled from dynamic measure probability map, together with a random sampling (e.g. Latin hypercube sampling) technique. We can take advantage of expanding our search space to cover the regions which dynamic measures might miss. We will show how our method identifies the optimal solution with faster convergence compared with normal genetic algorithm. The efficiency and practical applicability of our proposed approach is validated through synthetic and field infill well drilling optimization problems.

In Chapter III, we will present a new dynamic measure for fields under primary depletion. By consolidating the term ‘diffusive time of flight’ from Fast Marching Method into this dynamic measure, we get the proxy model for the genetic algorithm with hybrid sampling method. This new dynamic measure is validated through the well placement optimization problems in green fields. We also extend our approach to dual porosity models. In the dual porosity model, flow is assumed to be along the fracture

network and transfer between matrix and fracture. We expect to obtain better proxy models by incorporating mass transfer term, the flow between matrix and fracture to the dynamic measure.

In Chapter IV, a structured history matching approach which consists of global calibration and local calibration is applied to a field case. For the global calibration, our goal is development of multiple models which match the field-wide or regional performance. Key global parameters which heavily affect the model response such as bottom-hole pressure are selected through a sensitivity analysis. Design of experiments and response surface methodology with evolutionary algorithms such as genetic algorithm are used to calibrate these key global parameters. Then, local calibration using streamline based sensitivity and generalized travel time inversion technique is carried out to improve well by well match. We utilize streamline-derivative analytic sensitivities to determine the spatial distribution and magnitude of the local permeability changes.

CHAPTER II

WELL PLACEMENT OPTIMIZATION FOR WATERFLOODING USING DYNAMIC MEASURE PROBABILITY MAP WITH GENETIC ALGORITHM

2.1 Introduction

During the field development, finding optimal well locations is considered as one of the significant features to maximize its recovery or asset value. Dynamic measure based on the total streamline time of flight combined with static and dynamic properties can give us better idea where the remaining oil in the reservoir, since it incorporates unswept and undrained areas of oil from the streamline information. In addition, computation of dynamic measure is very efficient so that we can practically deal with large models with this streamline based method. However, the point with highest value of dynamic measure is not necessarily the optimal well location itself but it is expected to be close to well location.

In this chapter, we propose a method which utilizes the dynamic measure as a probability map and uses it as a proxy model for genetic algorithm. Previous work has shown us that a hybrid stochastic algorithm with proxy modeling generally converges to a reasonable solution with fewer evaluations compared to stochastic algorithms. Moreover, if we have a better proxy model, faster convergence will be obtained. Thus, building a response surface, which is a proxy model, from dynamic measure probability map enables us to reach the optimal solution more efficiently. The initial population sampled from the dynamic measure probability map is used for constructing initial

response surface. However, if we gain the initial response by random sampling (e.g. Latin hypercube sampling) combined with population sampled from dynamic measure probability map, we can take advantage of expanding our search space to cover the regions dynamic measures might miss. We show how our method identifies the optimal solution with faster convergence compared with normal genetic algorithm. In addition, it is also shown that we can avoid being trapped in local minima since we have sampled initial populations from the dynamic measure map, which is a good indicator of remaining oil. The efficiency and practical applicability of our proposed approach is validated through synthetic and field infill well drilling optimization problems.

2.2 Background

2.2.1 Application of Optimization Methods

Finding optimal well locations is one of significant features of the field development problems. In mature field, it is more complex to locate infill well drilling locations since there are many existing wells in addition to the heterogeneities in the reservoir. It is necessary to capture how the reservoir behaves to find optimal locations but it is harder to accomplish it in mature field. Well placement problems to be solved are expressed as optimization problems. Well placement optimization could be a problem of maximizing either oil recovery or asset value of the project. In general, the optimization problem of well placement is computationally expensive and it is required to deal with geologic uncertainty.

Many optimization techniques were introduced and used for various applications. In the reservoir management, well placement optimization is one of the most interesting areas. The optimization methods on well placement problems are traditionally categorized into deterministic and stochastic methods. However, in order to take the advantage of each algorithm, hybrid methods were implemented here.

2.2.1.1 Deterministic Methods

In the area of deterministic methods, descent algorithms were widely used with the adjoint methods to compute the gradients. Direct pattern search methods and simplex methods are also included in deterministic methods. Deterministic methods can converge very fast with high precision on the condition they are given a good initial guess for the global optimum. But if the initial guess is far away from the global optimum, they are likely to get trapped in local optima. To use deterministic methods, the model of the function should be necessarily smooth enough.

Sarma et al. (2008) calculated the gradient of an objective function, Net Present Value (NPV), with respect to x, y locations of wells using adjoint methods. They found optimal well location for a synthetic case but they knew that their method is likely to get caught in local minima.

Moreover, the adjoint methods are known for their implementation difficulties and needs to access to simulator source code. Because of these weakness, large scale field applications are limited with deterministic methods.

2.2.1.2 Stochastic Methods

Stochastic methods are based on generation of random variables. These methods have been introduced to mitigate the flaws of deterministic methods. To optimize the objective functions such as non-smooth and multi-modal, these methods are particularly useful. Particle swarm optimization (PSO), simulated annealing (SA), simultaneous perturbation stochastic algorithms (SPSA) and evolutionary algorithms (EA) are examples of stochastic methods.

Artus et al. (2006) used genetic algorithm for the placement of monobore and dual lateral wells. Emerick et al. (2009) also used genetic algorithm to optimized field development scenarios. Number of horizontal wells, their types and locations are the variables for the scenarios.

Typically, stochastic methods may require many more simulations than deterministic methods since stochastic methods rely on random generation and re-trials to identify the parameter intervals to obtain the optimal solution. However, even though stochastic methods are not computationally efficient to find the precise optimum, they generally have good ability to get closer to the global optimum.

2.2.1.3 Hybrid Methods

Hybrid methods are the combined methods from two or more algorithms to take advantage of the merits of each algorithm. Hybrid methods generally are designed to have the strong points from multiple algorithms, so the performance is better than each individual algorithm.

Bittencourt et al. (1997) used hybrid methods composed of genetic algorithm (GA), TABU and polytype algorithm for optimizing numbers of vertical horizontal wells. Guyaguler et al. (2002, 2004) optimized infill well drilling locations using the hybrid optimization scheme consisting of genetic algorithm (GA), artificial neural network (ANN), polytype algorithm and kriging. They found that GA with these helper methods reduced the computations, which is the number of simulation needed. The use of hybrid methods are also found in the work of Yeten et al. (2003). They used genetic algorithms with hill climbing algorithm to optimize well type.

To be more computationally efficient, search algorithms using proxy modelling are used. In the literature, proxy modelling are also called surrogates or meta-modelling. Proxy model is an approximate model which replaces the true objective function to reduce the number of simulations needed. Proxy model can be obtained from kriging with least squares, basis function, quality maps and multiple regression methods.

2.2.2 Dynamic Measure

Dynamic measure is a kind of quality maps which indicates oil producing potential in the reservoir. First, we go into quality maps and we will review the dynamic measure and its rationale in the following section.

2.2.2.1 Quality Maps

The reservoir quality maps are usually based on static and dynamic properties of the reservoir. Permeability, porosity and net thickness were used for static properties. On

the other hand, dynamic properties such remaining oil, well productivity, pressure and cumulative oil production of the reservoir were other components of the quality maps. The regions with high values on these quality maps are the interested areas for the well locations. The objective functions to be maximized in the well placement problems are typically cumulative oil or net present value (NPV).

Kharghoria et al. (2003) proposed the productivity potential maps to optimize well trajectory using heuristic methods. This map is the combination of static properties like porosity, permeability, dynamic properties such as oil saturation and geometric parameter, distance from well boundaries. Da Cruz et al. (2004) proposed quality maps, 2D representation of cumulative oil production. 3D maps were converted to 2D maps by the assumption that wells are perforated though all layers. They simulated some fraction of the reservoir and non-simulated cells got interpolation values from kriging. Liu et al. (2006) modified productivity maps proposed by Kharghoria et al. (2003) to include effective pore pressure and mobile oil saturation.

2.2.2.2 Review of Dynamic Measure

Dynamic measure was recently proposed by Taware et al. (2012). Like quality maps, it is composed of static and dynamic properties about remaining oil in the reservoir. Unlike previous quality maps which didn't consider some factors affecting field production, reservoir drive mechanisms, drainage and sweep areas, they added Total Time of Flight (TTOF) term to the dynamic measure. By adding total time of flight

(TTOF) of streamline simulation to the dynamic properties, structure of the reservoir, geometry of existing well patterns and drive mechanisms can be honored.

The rationale of the dynamic measure were explained as follows. Dynamic measure was derived heuristically. By definition, dynamic measure (DM) is the multiplication of static properties, permeability (k) and pore volume (PV) and dynamic properties such as oil saturation (S_o), oil relative permeability (k_{ro}) and the total time of flight (TTOF). All these properties are rank normalized to remove the influence of the absolute values of each property.

The dynamic measure is,

$$Dynamic\ Measure(DM) = (TTOF_{RN} \cdot So_{RN} \cdot porevolume_{RN} \cdot k_{RN} \cdot kro_{RN}) \qquad (2.1)$$

The rationale begins from the oil volumetric flux q_o. q_o for a given grid cell is,

$$q_o = PI \cdot \frac{kro(S_O)}{\mu_o(\bar{P}) \cdot B_o(\bar{P})} \cdot (\bar{P} - P_{wf}) \qquad (2.2)$$

Where PI is,

$$PI = \frac{k \cdot (\Delta z) \cdot (NTG)}{7.08 \cdot 10^{-3} \cdot \left[\ln\left(\frac{r_o}{r_w}\right) + S \right]} \qquad (2.3)$$

Where, $kro(S_o)$ is relative oil permeability at each grid cell. $\mu_o(\bar{P})$ is oil viscosity and $B_o(\bar{P})$ is oil formation volume factor. These are function of average reservoir pressure. Because one is interested in relative oil productivity for a given drawdown,

parameters common to the grid blocks such as $\mu_o(\overline{P})$ and $B_o(\overline{P})$ can be factored out (Kharghoria et al. 2003). Also, q_o represents volumetric oil flux and contains no information about the total oil volume associated with it. Hence, $\phi \cdot S_O$ is added to incorporate the oil volume (Kharghoria et al. 2003). Therefore, the dynamic measure can be heuristically represented as,

$$DM \cong \Delta z \cdot NTG \cdot \phi \cdot S_O \cdot k \cdot k_{ro}(S_O) \tag{2.4}$$

The oil bearing capacity $\Delta z \cdot NTG \cdot \phi \cdot S_O$ can be replaced by $porevolume \cdot S_O$. Total time of flight (*TTOF*) is the term highlighting the areas that are poorly drained and swept. Hence, the dynamic measure is computed as follows (Fig. 2.1),

$$Dynamic\ Measure\ (DM) = Porevolume \cdot S_O \cdot k \cdot k_{ro}(S_O) \cdot TTOF \tag{2.5}$$

Using rank normalization to remove the influence of absolute values of each property,

$$Dynamic\ Measure\ (DM) = (TTFT_{RN} \cdot So_{RN} \cdot Porevolume_{RN} \cdot k_{RN} \cdot kro_{RN}) \tag{2.6}$$

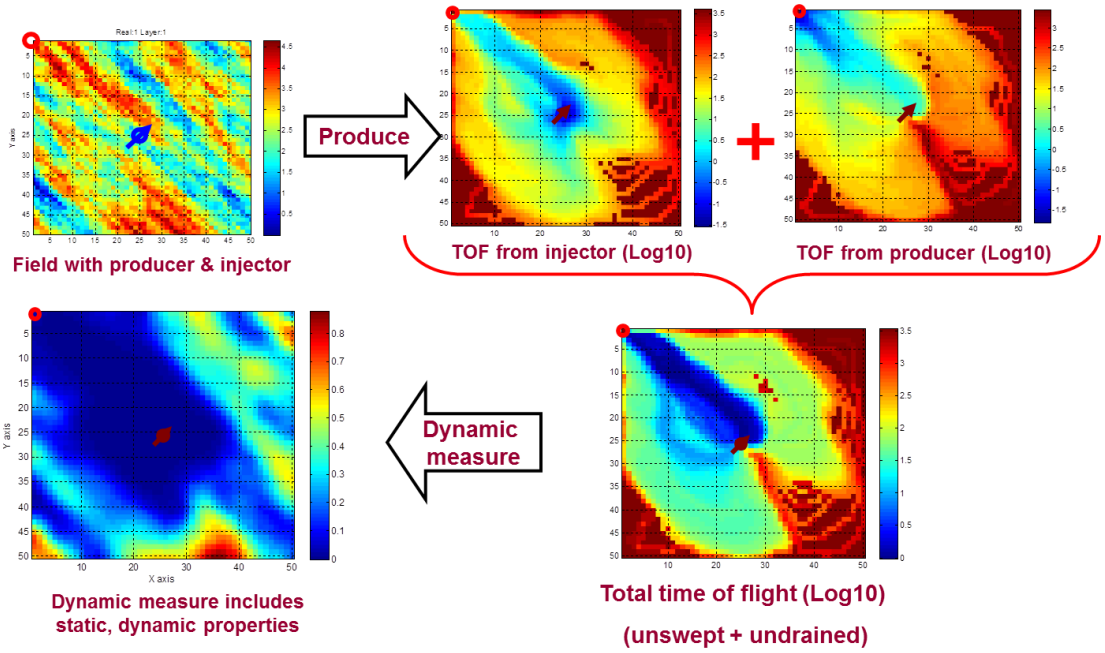

Fig. 2.1 Total time of flight (TTOF) in Dynamic Measure (Taware et al. 2012)

2.2.3 Evolutionary Strategy

2.2.3.1 Genetic Algorithm

As we reviewed in previous section, genetic algorithms are most widely used methods for derivative-free optimization. The genetic algorithm imitates the biological principles of evolution, survival of the fittest. The fitness of each individual is evaluated based on their performance, measured as a fitness function. The genomes or chromosomes, which are the full binary string containing all variables, start from a randomly generated population and multiple individuals are stochastically selected to be directly manipulated through crossover and mutation, to generate a new generation. For genetic algorithm, crossover is the dominant operator while mutation is mainly used for

keeping the genetic diversity of the population (Cheng et al. 2008). Commonly, the algorithm terminates when a satisfactory fitness level or the maximum number of generations has been reached.

In genetic algorithm, the parameters are generally expressed as binary strings of 0's and 1's, called genotype. When evaluating their fitness, the binary strings should be decoded into phenotype and then, the objective function can be calculated. Imitating the biological principles of evolution, which is the survival of the fittest, the parameter sets with smaller data misfit have larger fitness.

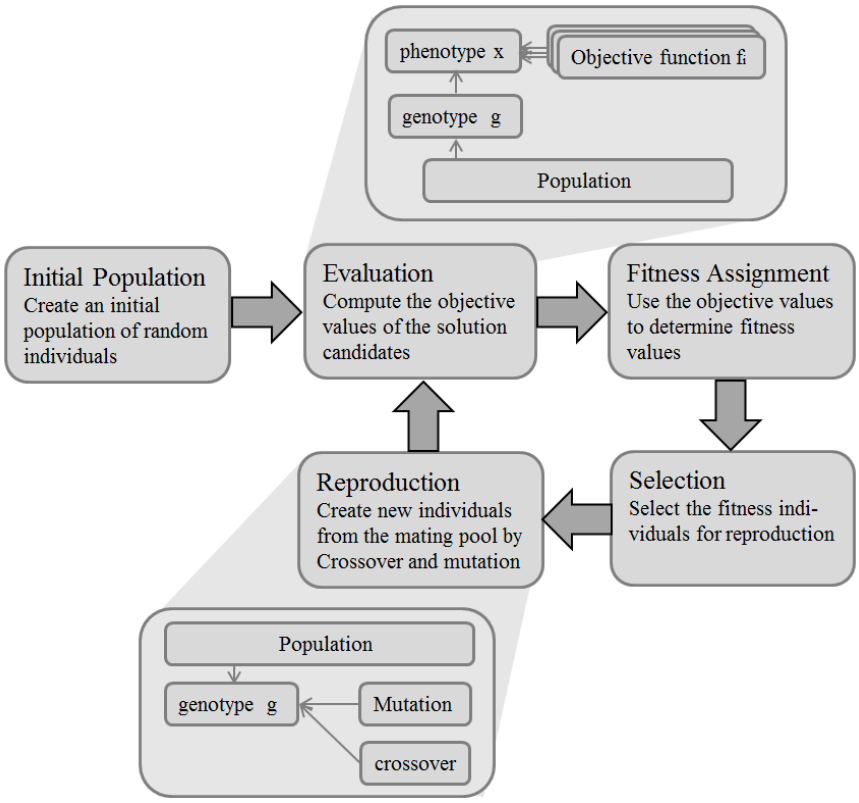

Fig. 2.2 The basic cycle of genetic algorithms (Weise 2008)

To start with, a diverse set of models comprising the initial population is created either randomly or within an experimental design framework (e.g. Latin hypercube sampling). The objective function of the current population is calculated, and then fitness values are assigned to each sample according to their objective values. The genetic algorithm selects a percentage of the population based on the value of fitness for breeding a new generation. The selection process is stochastic and random in nature. Genetic operators, mutation and/or crossover, are then utilized to reproduce a new generation. This process is repeated, as shown in Fig. 2.2

Crossover is the key process of creating new samples, or offspring, by recombining old samples. It is assumed that recombination of fitter parents will reproduce well and even better performing offspring, thus accomplishing the major objective of increasing the fitness function. This operator randomly chooses locations and exchanges the subsequences before and after those locations between two parameter vectors. There are typically three types of crossover operation, as shown in Fig. 2.3, single-point crossover, multi-point crossover and uniform crossover. For single-point crossover, one single position is randomly chosen and parents swap their binary bits with each other; in multi-point crossover, genome are partitioned into several segments and each of these segments (except for the first segment) take a crossover probability to swap with the same segment of the other genome; and for uniform crossover, each pair of bits form two parents will take a probability to swap. Generally speaking, the uniform crossover introduces diversity faster than multi-point or single-point crossover.

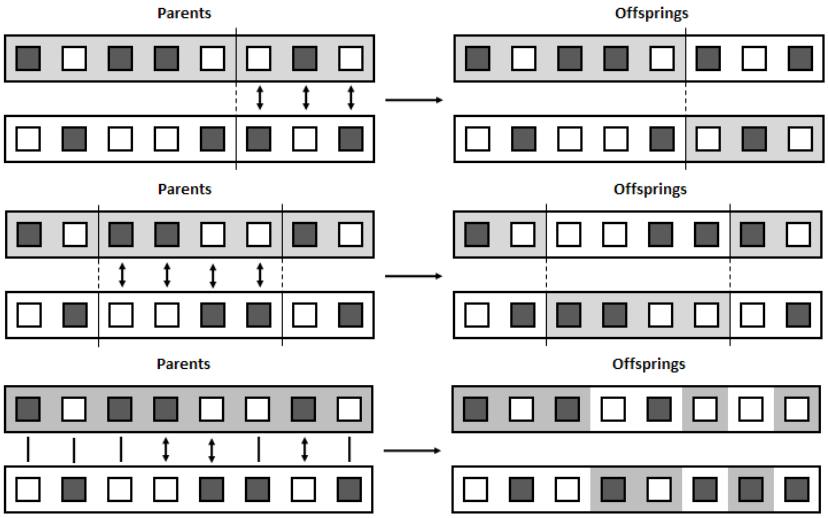

Fig. 2.3 (a) Single-point crossover; (b) Multi-point crossover; (c) Uniform crossover (from the top)

Mutation imitates "asexual" influences to a genome by, for example, environmental change. It is a key component to introduce new diversity to the generation though mutation is commonly paradoxical because most of them are harmful or at most neutral (Sawyer et al. 2007). This operator randomly flips some of the bits in binary form parameters (Fig.16). Mutation can occur at each bit position in a string with some probability, which is usually very small. The mutation step typically follows crossover for each combined sample of string. For an optimization process, most of the hill climbing is via crossover while occasional mutation forces trial over all space, providing chances to find the global optima.

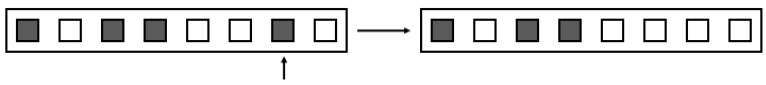

Fig. 2.4 Uniform mutation

2.2.3.2 Genetic Algorithm with Proxy Modelling

As we reviewed in previous section, hybrid methods are generally more efficient to find optimal solution. Guyaguler et al. (2004) showed hybrid stochastic algorithms with proxy modelling generally converge to reasonable solution with fewer evaluations compared to stochastic algorithms

For this research, we utilized our group's software, GLOBAL. The flowchart of GLOBAL is shown in Fig. 2.5. In order to more effectively select the large amount of samples proposed by genetic algorithm, a proxy model is used.

Experimental design is used to generate a response surface. Genetic algorithm generation are initialized and updated with genetic operators implemented. Instead of evaluating each sample by running simulation, the proxy checks samples before going to the simulation step. The proxy check process estimates the objective function value from the response surface. The samples, whose estimated values satisfy the fitness criteria, will proceed to simulation. Other samples that fails to pass the proxy check are discarded, making the genetic algorithm work more efficiently. After evaluating one whole generation, a converge criteria is checked. If the convergence is not satisfied, then these evaluated samples are added into the proxy pool, thus proxy is updated, and then the GA process is repeated until convergence or satisfactory reservoir models are found.

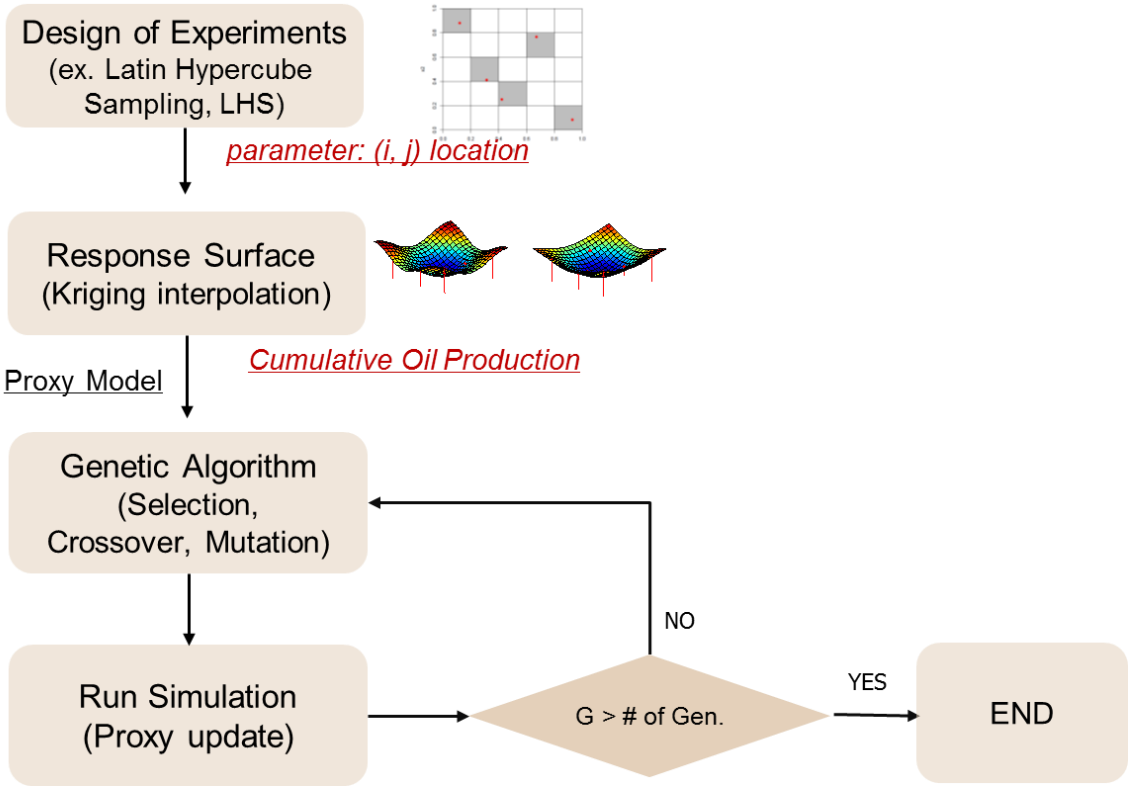

Fig. 2.5 Workflow of Hybrid Genetic Algorithm

2.3 Approach

The better proxy model that hybrid methods are combined with, the more efficiently the algorithms can find optimal solution. Dynamic measure combines static properties and dynamic properties including Total Time of Flight. It is a good indicator of where oil remains in the reservoir and provides a possible well new location. However, the point with the highest dynamic measure value is not necessarily the optimal location for additional well. Nevertheless, the point with maximum value of dynamic measure is reasonably expected to be close to the optimal well location.

We can take advantage of dynamic measure to reach the optimal solution more efficiently. If we sample candidate well locations from the dynamic measure map and construct response surface with these locations, we expect to get the optimal solution with fewer evaluations. We used dynamic measure as a probability map. It means the points with higher value has more possibility to be selected for the initial response surface. We built a response surface from this probability map and used with genetic algorithm.

We proposed two new approaches to obtain global optimum of the objective function. We will compare two new approaches in a later section with the simulation results and discuss what advantages our approach have over normal sampling. In this research, our objective function is cumulative oil production, however, we can solve this optimization problem for maximizing Net Present Value (NPV) also.

2.3.1 Dynamic Measure Sampling

In our first proposed approach, we sampled candidate well locations from the dynamic measure probability map according to their values. It is more probable that the cells with higher dynamic measure value are sampled for candidates. Then we constructed response surface for the genetic algorithm (GA) with the initial candidate well locations whose parameters are (i, j) locations in the reservoir model. Then, we updated the well locations using this response surface with genetic operators such as crossover, mutation and replacement. We called this proposed approach as ‘genetic

algorithm (GA) with Dynamic Measure (DM) sampling'. The workflow is shown in Fig. 2.6.

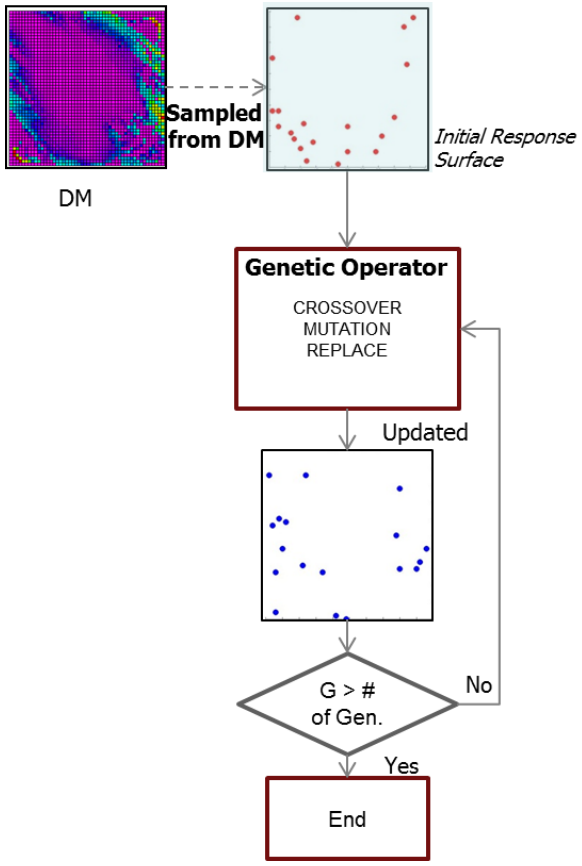

Fig. 2.6 Workflow of Genetic Algorithm with Dynamic Measure Sampling

2.3.2 Hybrid Sampling

Second, we proposed a hybrid sampling scheme for the initial response surface. This approach is different from the first proposed approach in the way of sampling candidate well locations for the initial response surface. In this approach, we construct the initial surface from the initial population by random sampling together with the

initial population from the dynamic measure probability map (Fig 2.7). By adding this random sampling to dynamic measure sampling, we expect to expand the searching space that the dynamic measure might miss. We just added small number of initial candidate well location so as not to sacrifice computational efficiency. In our research, we sampled equal number of candidate well location from dynamic measure probability map and random sampling. We will show why we need this hybrid sampling with an example in a later section.

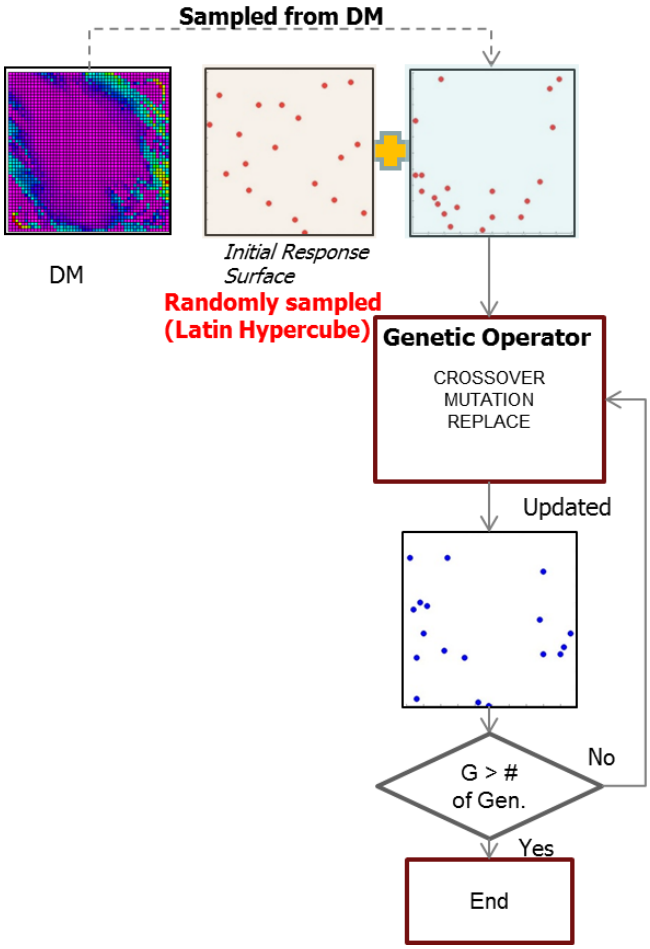

Fig. 2.7 Workflow of Genetic Algorithm with Hybrid Sampling

2.4 Application

2.4.1 Synthetic Case

First, we applied our workflow to a 2D synthetic model case. The dimension of the model is 50 by 50 and we assumed a 2 phase, oil and water, reservoir. One producer and one injector were initially drilled as shown in Fig. 2.8. Producer was placed in upper left corner and injector is located at the center of the reservoir. In this model, oil has been produced for 2,000 days and we want to find the optimum infill well location for maximizing total cumulative oil production at 4,000 days.

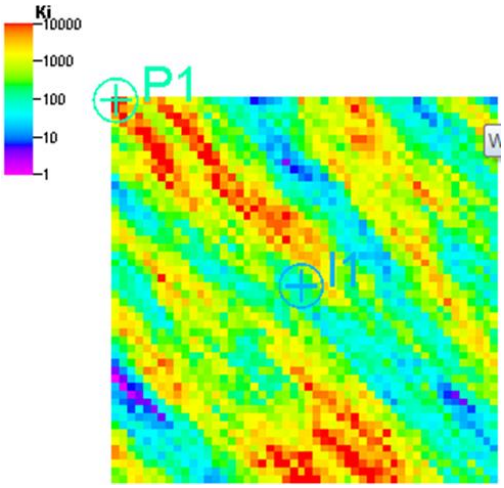

Fig. 2.8 Permeability distribution of a synthetic case

As explained, dynamic measure map is obtained from one single reservoir simulation. From this simulation, we got all property values for each grid cell and combine these properties to get dynamic measure value for all possible well locations.

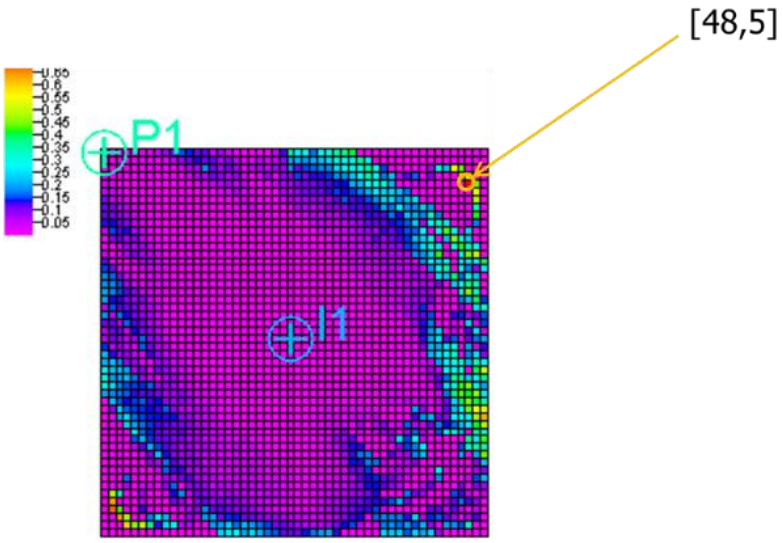

Fig. 2.9 Dynamic Measure map for 2-D synthetic case

Fig. 2.9 shows the results of dynamic measure map for 2-D synthetic case. As shown in the figure, the location with the maximum values is in the upper right part of the reservoir.

To compare the dynamic measure map with the actual simulation results, we ran about 2,500 (50 by 50) simulations for all possible candidate well locations and obtained cumulative oil production values for each cell. We called this map as exhaustive calculation map since these simulations covered all the grid cells. Fig. 2.10 showed us the total oil production for all possible well locations. As shown in the figure, the maximum total oil production is obtained in the upper right part of the reservoir. Both the location of the highest dynamic measure value and the optimum well location from exhaustive simulation results are in the upper right of the reservoir and these two locations are fairly close.

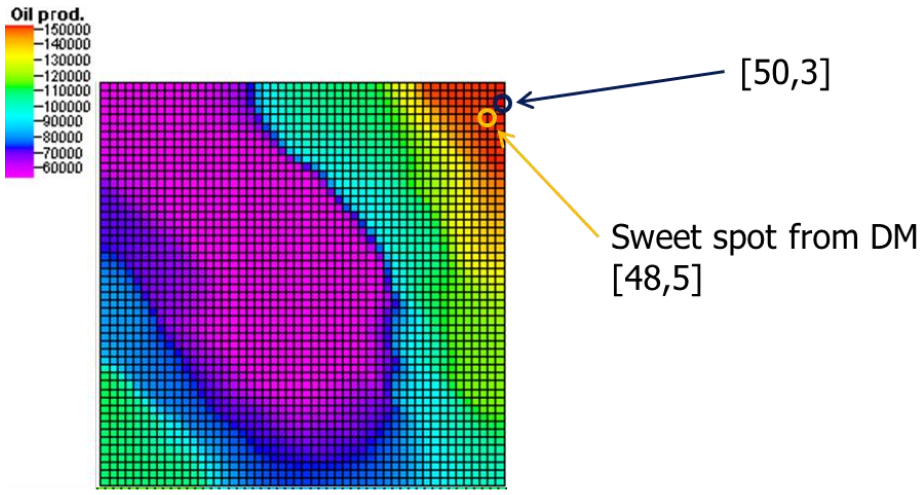

Fig. 2.10 Exhaustive Calculation Map shows Total oil production for all candidate well locations at 4,000 days

But, when we look at the overall trends of dynamic measure map and exhaustive calculation map (Fig.2.10), we find the correlation between the two maps is not so strong. It means the overall trends are similar but a bad location of the dynamic measure map is not necessarily a bad spot in actual simulation results. Dynamic measure map itself can be a good starting point for locating best well location, it would be more accurate with the help of randomness.

We optimized well placement problems with three approaches and compared one another. Firstly, we ran the genetic algorithm with random sampling, Latin Hypercube Sampling (LHS) in this research, of initial population to construct response surface. Secondly, we sampled initial population from dynamic measure probability map and genetic algorithm was used also. Thirdly, we construct initial response by random sampling and dynamic measure sampling.

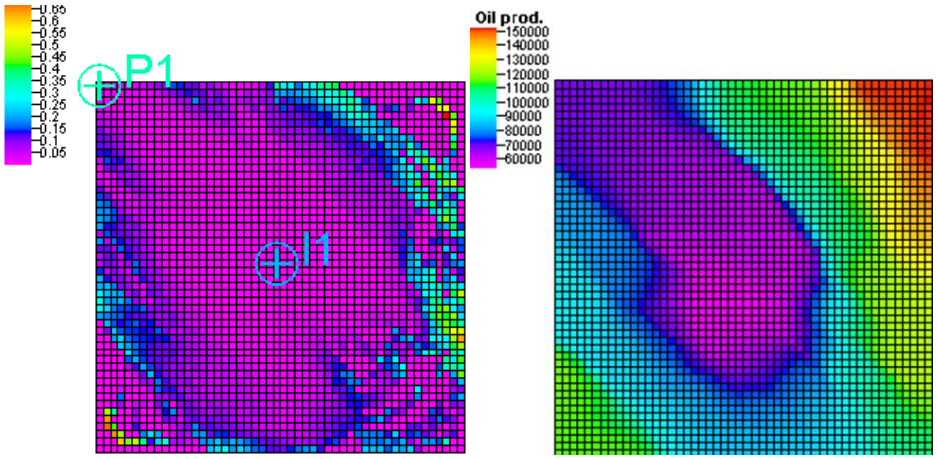

Fig. 2.11 Comparison between dynamic measure map (on the left) and exhaustive calculation map (on the right)

Fig. 2.11 shows the results of each approach. The red circles represents the region around optimal solution. For the case of first approach, we might miss the optimal solution if we don't provide enough randomness to genetic algorithm. The result of first approach in Fig. 2.12 is an example of missing the optimal solution. Generally, genetic algorithm is known to be useful for solving multi-modal and non-smooth problems, but we need to sacrifice computational efficiency to get the optimal solution. Even though genetic algorithm is combined with proxy model, there is trade-off between the quality of proxy model and the computational cost of the optimization. So, if we want to find optimal solution with less simulation (i.e. the number of population for the genetic algorithm needs to be small), then we need better proxy model than the one from random sampling.

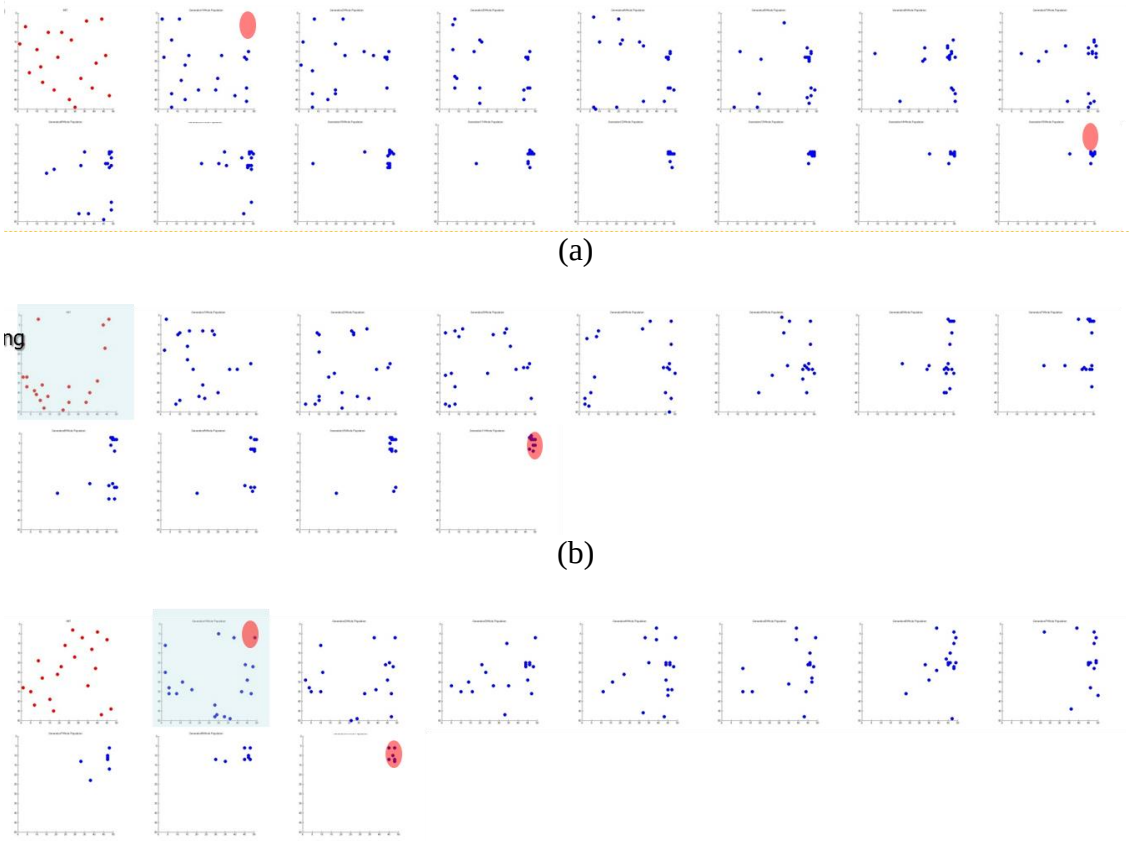

(a)

(b)

(c)

Fig. 2.12 An example of results from sampling techniques

The second approach shows that the algorithm converges to the optimal location. Red dots in each approach are initial population which are candidate well locations and blue colored means that the candidate well locations come from the dynamic measure sampling. If we look at the initial population of second approaches, we can find the initial candidate well locations are mostly distributed on the spots which we can get higher total oil production (Fig. 2.12). It means that we don't need lots of generations for

genetic algorithm and can save lots of simulation since we have initial populations close to optimal solution.

For the third approach, we have two initial population coming from random and dynamic measure sampling which are depicted in first and second map in Fig.2.12 (c) respectively. We add randomness to our first proposed approach by randomly sampling initial candidate well locations. As shown as in blue colored picture of Fig. 2.12 (c), we obtained a candidate location which is in the vicinity of optimal location for the initial population with the help of dynamic measure sampling. It enabled genetic algorithm to start searching from better locations. Also, we got more information from the wells sampled from random sampling.

2.4.2 Field Case

We applied our proposed approaches to a field case model whose dimension is 58 by 53 by 10. This reservoir is a mature field in which there are 33 producing wells and 10 water injecting wells. The objective function is total oil production and we calibrate the location of a new infill well to achieve maximum total oil production. A vertical well is drilled at 3,840 days and dynamic measure probability map was generated from the simulation result at 3,840 days. Fig 2.13 shows the permeability distribution of the field.

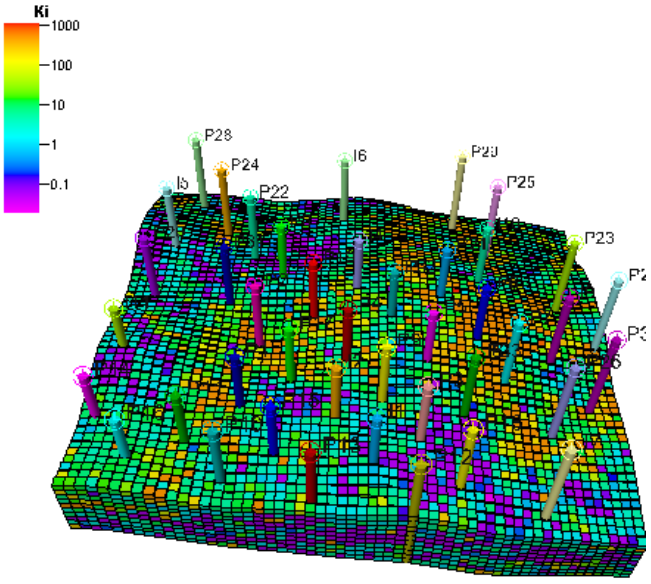

Fig. 2.13 Permeability distribution of water flooding field

For this field case, we assumed a vertical well which is perforated all along the k direction, so the value of each grid (i, j) is summed up in the k direction. Dynamic measure map in Fig. 2.14 is depicted as 2D by the summation. The picture on the right in Fig. 2.14 show that we can get the optimal well location in the upper right part of the field. The good points on the dynamic measure probability map correlate to total oil production on the right except for the points in the top edge. From this point, the initial response surface by random sampling is necessary to expand the search space to the regions like top edge of the reservoir.

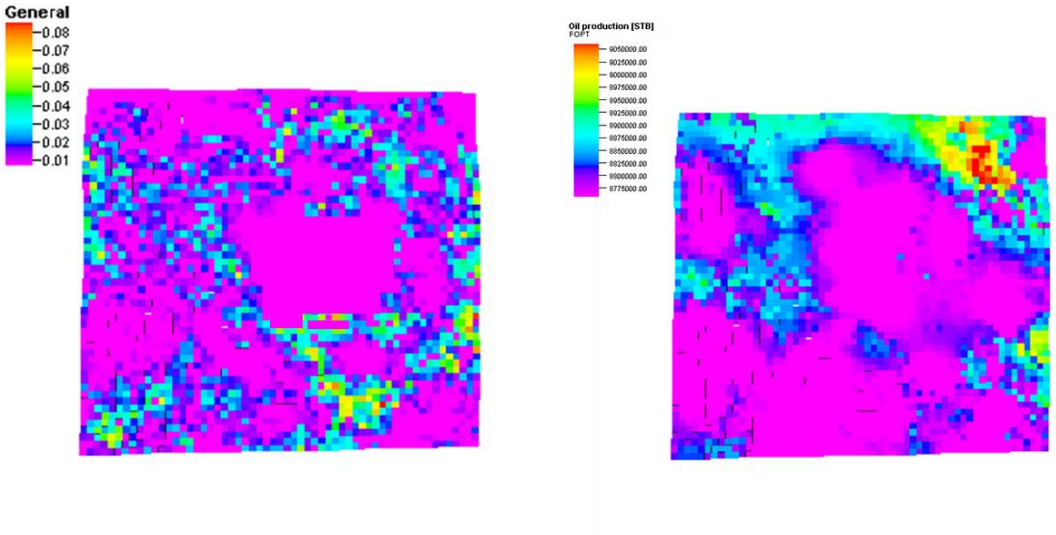

(a) (b)

Fig. 2.14 (a) Dynamic measure probability map; (b) Total production from exhaustive calculation

Fig. 2.15 shows the result of each approach. As the results in synthetic case, our proposed approaches gives good convergence with fewer evaluations. In a previous section, there is no significant difference between the results of dynamic measure sampling and hybrid sampling (Fig. 2.12). For this field case, the correlation between dynamic measure and total oil production results is not strong as the synthetic case in previous section. Dynamic measure probability map provide with good starting points by itself, but initial candidate well locations by random sampling can give us good information dynamic measure might miss.

As shown in Fig. 2.15, hybrid sampling gave good convergence with fewer simulations compared to dynamic measure sampling technique. The advantage of hybrid sampling technique can be summarized as follows:

(1) Since it is based on genetic algorithm method, it can avoid being trapped in local minima if it has sufficient number of populations.

(2) Combined with proxy modelling, it can converge to reasonable solution with fewer evaluations. Dynamic measure probability map is a good source of proxy model for the genetic algorithm so that it reduces the number of simulations to reach optimal solution.

(3) Hybrid sampling technique can provide more efficiency compared to dynamic measure sampling only when dealing with more complex case.

Fig. 2.15 An example of results from sampling techniques

From the study of synthetic and field cases, we found that the correlation between dynamic measure and total oil production in the field case appears not as strong as the synthetic cases. If we compare the possibility that the population sampled from dynamic measure hit the upper 20% rank of actual total production location, the field case shows about 40 to 50 % level of the synthetic case. We can think this is because the reservoir responses get more complex for field cases and even more complicated with drilling more wells during the field development.

Also, we found that oil saturation and oil relative permeability tend to show better correlation with actual simulation results than total time of flight for the reservoir in early stage with less number of wells, whereas total time of flight better contribute to the correlation in the relatively mature reservoir with many wells. More detailed and quantitative study might be necessary to analyze the contribution of each parameter to the correlation for more types of reservoir. However, parameters can play their roles more effectively when they are combined one another.

For 3D cases, we summed up dynamic measure value along the k direction and generated 2D map for the well placement because we consider a vertical well case. It means that we choose arithmetic average of dynamic measure in a column. We might use geometric average, but the dynamic measure map generated using geometric average usually shows worse correlation with the simulation results (Figure 2.16).

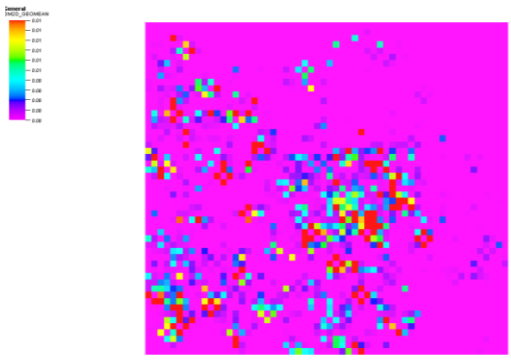

Fig. 2.166 Dynamic measure using geometric average along k direction

2.5 Summary and Conclusions

In this chapter, we proposed a hybrid sampling workflow using genetic algorithm and response surface, to obtain the global optimum solution for the well placement problems. Dynamic measure which is an indicator of remaining oil in the reservoir is combined with the hybrid sampling method and used as proxy model for the well placement optimization.

Our workflow is based on hybrid optimization method in which genetic algorithm is associated with proxy modelling. Genetic algorithm proved to be a good tool for the well placement optimization. We can take advantage of avoiding being trapped in local minima using genetic algorithm.

Candidate well locations from dynamic measure sampling technique is used to construct response surface to search the optimal well location. Proxy model sampled from dynamic measure probability map enabled genetic algorithm to converge to optimal solution with fewer evaluation.

Hybrid sampling method is a combined sampling technique composed of dynamic measure sampling and random sampling. Randomly sampled candidate well locations can cover the region dynamic measure sampling might miss. Hybrid sampling method is considered to be more efficient than dynamic measure sampling.

CHAPTER III

WELL PLACEMENT OPTIMIZATION FOR GREEN FIELD USING FAST MARCHING METHOD

3.1 Introduction

Contrary to the reservoirs which have matured to a production plateau or been declining and need fluid injection for improved recovery, primary depletion reservoirs, known as green fields, are mainly dependent on pressure depletion from producing wells. For primary depletion field, we can take advantage, in term of cost of computation, of using Fast Marching Method with which we can get diffusive time of flight. This diffusive time of flight term is analogous to convective time of flight in streamline simulation.

The depth of investigation is defined as the propagation distance of peak pressure disturbance for an impulse source. By using asymptotic expansion of the diffusivity equation, we can obtain the propagation of the pressure front for heterogeneous reservoirs, which is in the form of an Eikonal equation. We can solve this equation with Fast Marching Method and get a diffusive time of flight at each and every cell within the domain. The advantage of using the Fast Marching Method is that we can get the frontal propagation very fast with a single non-iterative calculation.

By consolidating the diffusive time of flight from Fast Marching Method into a new proposed dynamic measure for primary depletion field, we can get the proxy model for the genetic algorithm with hybrid sampling which is proposed in the previous chapter.

This new dynamic measure which is for the primary depletion field is validated through the well placement optimization problems in green field.

We also extended our approach to dual porosity models. In dual porosity model, flow is assumed to be along the fracture network and between matrix and fracture. By incorporating mass transfer term which is the flow between matrix and fracture to the dynamic measure, we can derive an improved proxy model to get the optimal solution for the well placement problem in dual porosity model.

3.2 Background

We first review pressure front propagation equation from the depth of investigation and the fast marching method (FMM) which is a single-pass method. FMM is used to solve the Eikonal equation which is derived from the diffusivity equation.

3.2.1 Propagation of Pressure Front

Lee (1982) defined that 'radius of investigation' is the propagation distance of a 'peak' pressure disturbance for an impulse source or sink. In heterogeneous reservoir, the pressure front is not expected to be uniform in all directions, so the "depth of investigation" is introduced in lieu of "radius of investigation". To obtain the depth of investigation, an asymptotic solution for the diffusivity equation has been obtained (Vasco et al. 2000; Datta-Gupta and King 2007; Kim et al. 2009).

The followings are the derivation of the pressure front propagation. We start from the multi-dimensional diffusivity equation for a heterogeneous system,

$$\phi(x)\mu c_t \frac{\partial p(x,t)}{\partial t} = \nabla.\left(k(x)\nabla p(x,t)\right) \tag{3.1}$$

where, $\phi(x)$ is porosity and $k(x)$ is permeability. We assumed constant fluid properties, viscosity (μ) and compressibility (c_t).

By applying a Fourier transform to this equation, it becomes the following in the frequency domain:

$$\phi(x)\mu c_t(-i\omega)\tilde{p}(x,\omega) = k(x)\nabla^2\tilde{p}(x,\omega) + \nabla k(x).\nabla\tilde{p}(x,\omega) \tag{3.2}$$

The asymptotic solution to this equation can be obtained by considering the following pressure solution in terms of inverse powers of $\sqrt{-i\omega}$.

$$\tilde{p}(x,\omega) = e^{-\sqrt{-i\omega}\tau(x)}\sum_{j=0}^{\infty}\frac{A_j(x)}{\left(\sqrt{-i\omega}\right)^j} \tag{3.3}$$

where, $\tau(x)$ is the diffusive time of flight denoting the propagation time of the pressure front, and $A_j(x)$ is the pressure amplitude at the j-th order. The leading order high frequency term in the asymptotic expansion determines the pressure front propagation as shown below,

$$\tilde{p}(x,\omega) = A_o(x)e^{-\sqrt{-i\omega}\tau(x)} \tag{3.4}$$

By substituting this solution in Eq. (3.4) and collecting the terms with the highest order of $\sqrt{-i\omega}$. Eq. (3.5) can be obtained for the pressure front propagation.

$$\sqrt{\alpha(x)}\left|\nabla\tau(x)\right| = 1 \tag{3.5}$$

Where, α(x) is diffusivity term and is defined as,

$$\alpha(x) = \frac{k(x)}{\phi(x)\mu c_t} \tag{3.6}$$

Equation (3.5) is in the form of an Eikonal equation. It implies that the pressure front propagates in the reservoir with a velocity of the square root of diffusivity, α(x). Diffusive time of flight, τ(x) has the unit of square root of time which is consistent with scaling behavior of pressure diffusion. The pressure front propagation only depends on reservoir properties and fluid properties. Flow rates are not related with pressure front propagation.

3.2.2 Fast Marching Method

After deriving the pressure front propagation equation in the Eikonal equation form, the next step is how to solve this Eikonal equation efficiently. Instead of computing the diffusive time of flight by integrating along the pressure trajectories, we introduced a class of front tracking method, called the fast marching method (FMM) (Sethian 1999) to calculate the values of $\tau(\vec{x})$. FMM is a single-pass method utilizing the concept that $\tau(\vec{x})$ for the first-order PDE depends only on the value of τ along the characteristics passing through the point $\vec{x}$ (Sethian 1996). Thus, the solution of τ can be constructed in an

orderly one-pass fashion from smaller values of τ to larger values. The basic framework for the fast marching method is as follows (Sethian 1999):

(1) Label all grid nodes as unknown;

(2) Assign τ values (usually zero) to the nodes corresponding to the initial position of the propagating front and label them as accepted;

(3) For each node that is accepted, locate its immediate neighboring nodes that are unknown and label them as considered;

(4) For each node labeled considered, update its τ value based on its accepted neighbors using the minimum of local solutions of Eq. (3) discussed later;

(5) Once all nodes labeled considered have been locally updated, we pick the node which has the minimum τ value among them and label it as accepted;

(6) Go to step (3) until all nodes are accepted.

In a 5-stencil Cartesian grid, these steps are illustrated in Fig. 3.1. We put the initial source point for the propagating front and label it as *accepted* (solid red circle) as shown in (a). Then its immediate neighbors A, B, C, and D are marked as *considered* (circle), and the diffusive time of flight τ it takes for the pressure front to arrive at these four points are updated as shown in (b). The numbers on the lines indicate the diffusive time of flight τ it takes for pressure to propagate between the two adjacent nodes and the numbers inside the circles are the cumulative τ for the pressure to propagate to these nodes from the source.

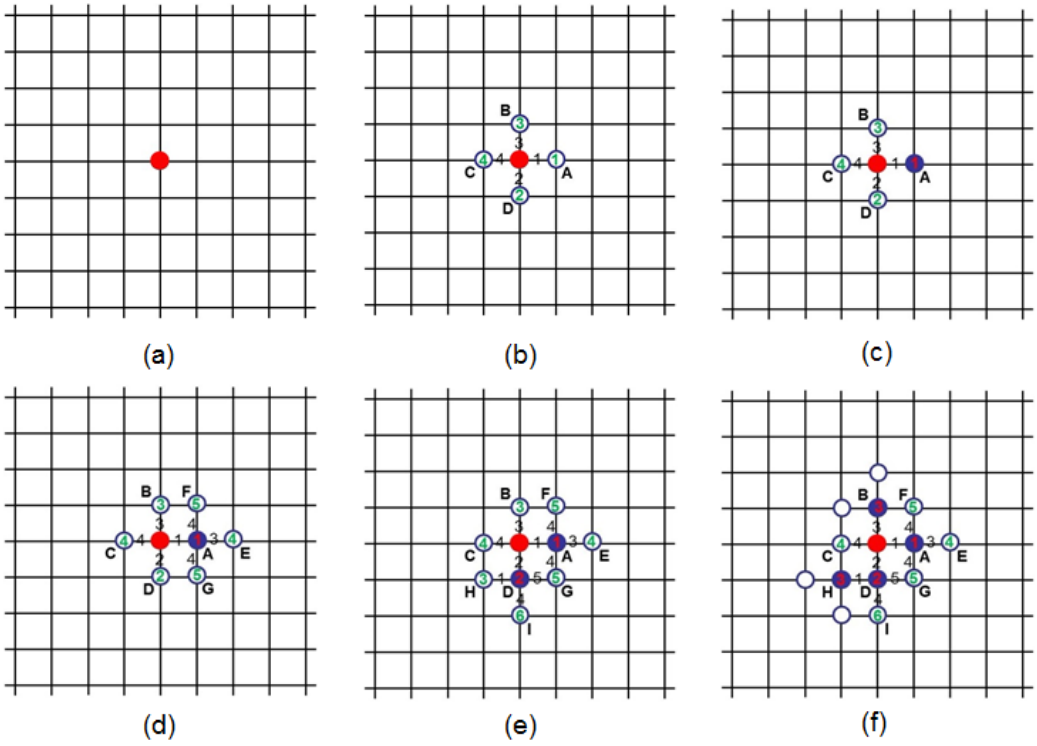

Fig. 3.1 Illustration of FMM in 5-stencil Cartesian grid

We pick up the smallest one (point A in this case), and make it as accepted as show in (c). Then its neighbors E, G and F are added into the considered and the τ for them will be updated as shown in (d).These steps will repeat for the next accepted point (like point D and then point H) as shown in (e) and (f). Basically, each time the new accepted point comes from the considered pool and has the smallest value of τ among all the considered points. If more than one point has the same smallest value of τ , we just accept them all at the same time. This process is repeated until the pressure front propagates the entire field. For 5-stencil Cartesian grid, we can directly update the cumulative τ value by writing Eq. 3.7 in a standard finite difference notation as (Sethian 1996):

$$\max\left(D_{ij}^{-x}\tau, -D_{ij}^{+x}\tau, 0\right)^2 + \max\left(D_{ij}^{-y}\tau, -D_{ij}^{+y}\tau, 0\right)^2 = \frac{1}{\alpha} \tag{3.7}$$

Here, the standard finite difference operator D for $\pm x$ directions can be written as $D_{ij}^{-x}\tau = (\tau_{i,j} - \tau_{i-1,j})/\Delta x$ and $D_{ij}^{+x}\tau = (\tau_{i+1,j} - \tau_{i,j})/\Delta x$. Similar equations hold for $\pm y$ directions. In Eq.6, τ values at *unknown* points are regarded as infinity and the "max" function is used to guarantee the "upwind" criteria. Eq. 6 leads to a quadratic equation and its minimum positive root gives us the τ value at point (i, j).

Alternatively, for a lattice we can calculate the τ values from each of the four quadrants (bottom-left, bottom-right, top-left, and top-right) and take the minimum τ value obtained. To locally calculate the diffusive time of flight it takes for front to propagate between two nodes separated by δr, we can just use the following expression.

$$\delta\tau(\vec{x}) = \sqrt{\frac{\phi(\vec{x})\mu c_t}{k(\vec{x})}}\delta r \tag{3.8}$$

3.3 Dynamic Measure for Green Field

In the previous chapter, dynamic measure is defined as the rank normalization of the static properties and the dynamic properties including Total Time of Flight (TTOF) of streamlines. For the green field case which is primary depletion reservoir, pressure best depicts the dynamic response of the reservoir. Consequently, diffusive time of flight term can take the place of convective time of flight term applied to water flooding, for the well placement optimization of green field case. It is easily understood because

diffusive time of flight is a direct analogue for diffusive processes of convective time of flight, which provides the underlying technology for streamlines.

As we reviewed in previous section, fast marching method is a very efficient tool to calculate the pressure front from source or sink. Therefore, we can get the value of diffusive time of flight in each and every grid cell from fast marching method. Like the time of flight of streamlines, the values of diffusive time of flight in cells give us the idea of where more hydrocarbon is remaining.

Our proposed new dynamic measure is also composed of static and dynamic properties. Permeability and pore volumes are included in static properties and diffusive time of flight is used for dynamic measure. Other dynamic properties such as hydrocarbon saturation and its relative permeability are not considered here. It is because we assumed our reservoir model is single-phase and also has uniform saturation for the simplification purpose.

So, the dynamic measure for green field using fast marching method is expressed as follows,

$$Dynamic\ Measure\left(DM\_FMM\right) = \left(DTOF_{RN} \cdot PoreVolume_{RN} \cdot k_{RN}\right) \qquad (3.9)$$

And, we obtain dynamic measure values for all grid cells.

We have also attempted other approaches to implement dynamic measure with fast marching method using drainage volume calculation. These are described in the Appendix C.

3.4 Application to Green Field

We applied our new dynamic measure (DM_FMM) to a primary depletion reservoir. The field model in Chapter II was modified for the green field simulation. We assumed an undersaturated oil reservoir model with two existing producers. Our objective function is to maximize cumulative oil production by placing a new vertical well in the optimal location. The permeability of the field is shown as below (Fig. 3.2).

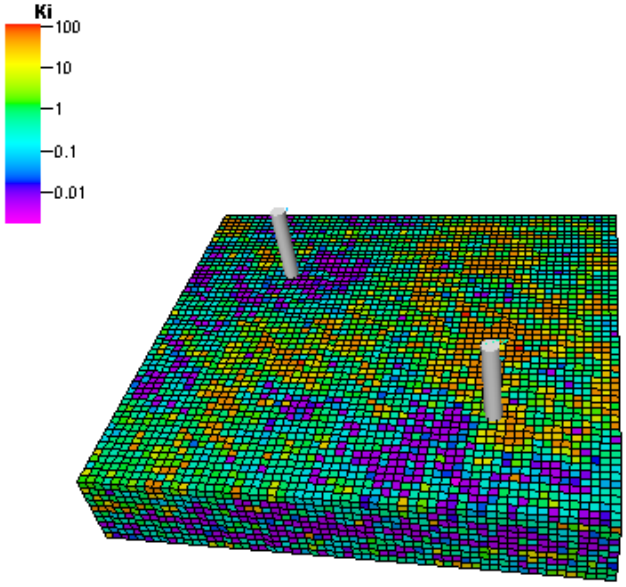

Fig. 3.2 Permeability distribution of the green field

Existing wells are assumed to be drilled initially and a new vertical well is to be drilled at 400 days. In this model, the diffusive time of flight (DTOF) is calculated from the existing two wells. DTOF value for each cell takes the minimum value of the values obtained from two existing wells.

We assumed a vertical well which is perforated all along the k direction for this research. Therefore, the value of each grid (i, j) is summed up in the k direction as is in the previous chapter. Dynamic measure map in Fig. 3.3 (a) is the 2D representation of the summation of dynamic measure. We also ran the simulation for every possible candidate well location with commercial reservoir simulator for the purpose of comparison with dynamic measure map. The optimal well location is located in the upper part of the reservoir (Fig. 3.3(b)).

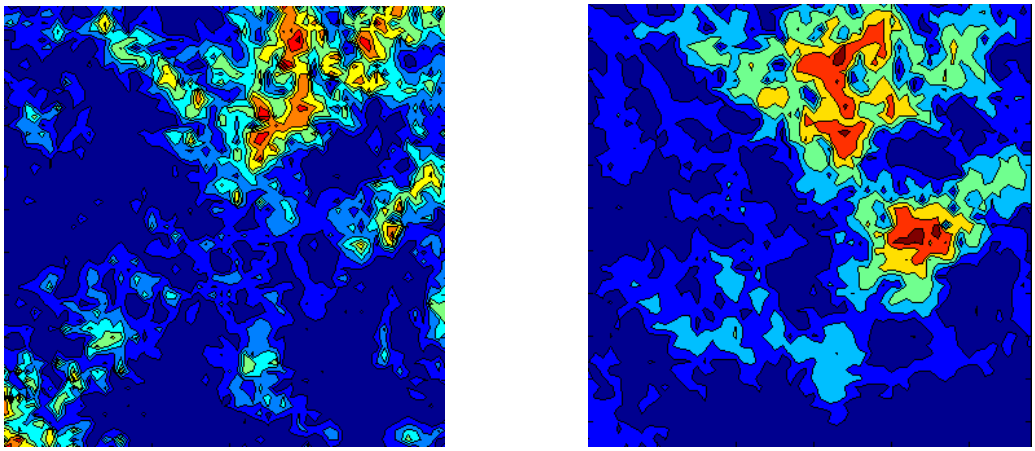

(a) (b)

Fig. 3.3 (a) Dynamic measure (b) Total oil production from exhaustive calculation

Fig. 3.4 shows the convergence of candidate well location for random sampling method and hybrid sampling method. The second picture of Fig. 3.4 (b) represents the candidate well location using dynamic measure sampling. The correlation between dynamic measure and total oil production obtained from exhaustive simulation is fairly

good (Fig. 3.3) in this case. Therefore, some initial candidate wells sampled from dynamic measure probability map are very close to the optimal solution.

Fig 3.4 (a) shows an example that random sampling method with small number of population can converge to local optimal location. To avoid this, genetic algorithm needs more initial population which results in increasing in the computational expenses. By using hybrid sampling method, genetic algorithm can converge with fewer simulations while avoiding local optima problem as shown as Fig. 3.4(b).

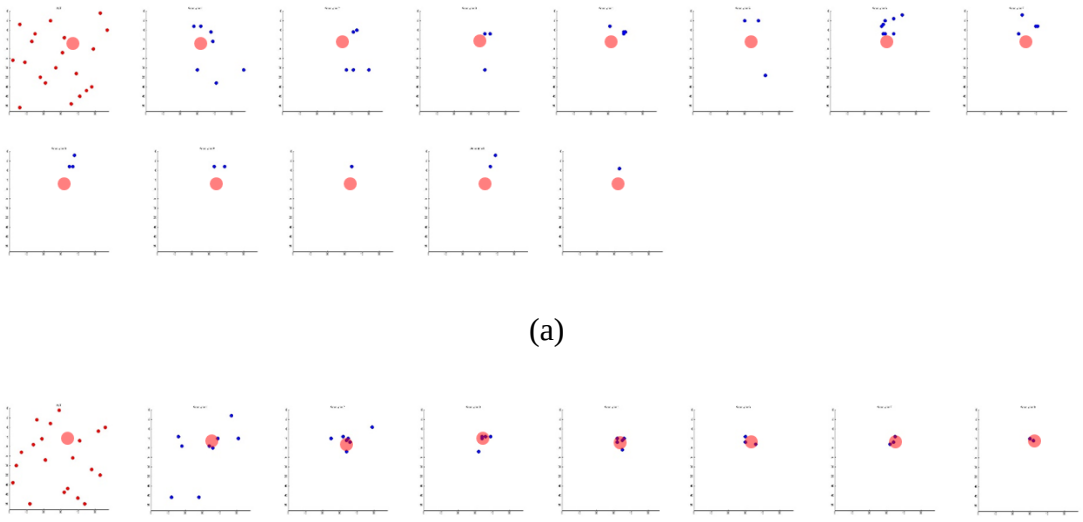

(a)

(b)

Fig. 3.4 Comparison the results of (a) random sampling and (b) hybrid sampling

3.5 Application to Dual Porosity Model

3.5.1 Review of Dual Porosity Model

Naturally fractured reservoir is characterized by a presence of two distinct porous systems which are fractured porous networks and fine grained matrix blocks. In naturally fractured reservoirs, the mass transfer between matrix and fracture is an important component due to their geological characteristics. While the matrix system has low conductivity with large storage capacity relative to the fracture, the fracture network has high conductivity with very little storage because of its very low porosity. The concept of dual porosity and single permeability (DPSP) model is comes from that the two overlapping continua, which are fracture system and matrix system, exist and interact each other (Warren and Root 1963, Kazemi 1979). The fluid transport equation in the fracture system is given by an ordinary porous medium with an additional connection to the matrix block, whereas the matrix blocks act only as a source to the fracture system.

Dual porosity modeling is computationally inexpensive compared with the Discrete Fracture Network (DFN) method which incorporates all fractures with complex fracture geometries. Fig. 3.5 are the illustrations of the fracture geometries in actual reservoir and the simplified grid block geometries in the dual porosity model. The dual porosity modeling has been traditionally utilized to model the fluid flows on the various scale medium using two simple coordinate systems (Blair 1964, Kazemi et al. 1979, Dean and Lo 1988).

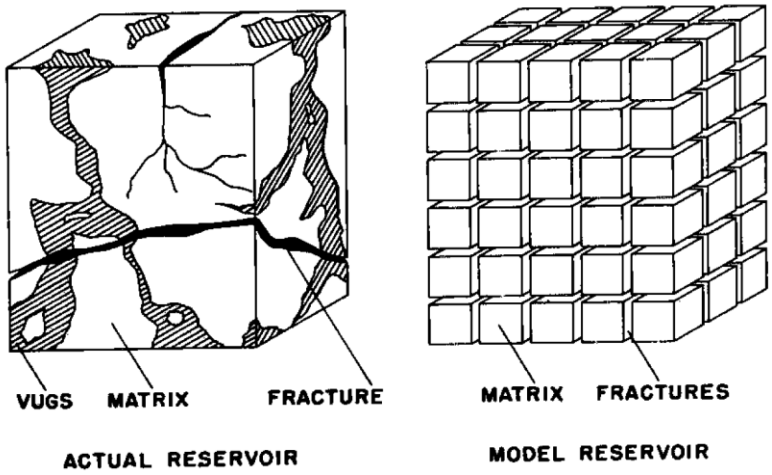

Fig. 3.5 Discretization of the fractured porous medium (Warren and Root 1963)

Warren and Root (1963) used pseudo-steady state equation to complete the dual porosity formulation. Their mass balance equation in the fractured system is expressed as a general mass balance equation with a matrix-fracture mass exchange term (Eq.3.10).

$$\frac{\partial(\rho\phi_f)}{\partial t} = \nabla \bullet \left(\rho \frac{k_f}{\mu} \nabla P_f\right) - \rho\Gamma + \rho q_f \tag{3.10}$$

where ϕ_f represents the fracture porosity, k_f denotes the fracture permeability, and Γ represents the matrix-fracture volume transfer function. The sink or source term q_f is imposed on the inner boundary condition of the fracture flow equation.

The transfer function is given by the Darcy equation-like form (Kazemi et al. 1976) as follows,

$$\Gamma = \sigma \frac{k_m}{\mu_{up}} \left(P_f - P_m\right) \tag{3.11}$$

where σ denotes the shape factor (fracture density) that defines the connectivity between the matrix block and the surrounding fracture network. It is reasonable assumption that the matrix-fracture volume transfer is always governed by the matrix permeability (k_m) due to its low conductivity

The flow equation for fracture system is,

$$\frac{\partial(\rho\phi_f)}{\partial t} = \nabla \bullet \left(\rho \frac{k_f}{\mu} \nabla P_f\right) - \sigma\rho \frac{k_m}{\mu}\left(P_f - P_m\right) + \rho q_f \tag{3.12}$$

And, the matrix flow equation is,

$$\frac{\partial(\rho\phi_m)}{\partial t} = \sigma\rho \frac{k_m}{\mu}\left(P_f - P_m\right) \tag{3.14}$$

where ϕ_m and k_m represent the matrix porosity and permeability, respectively. On the matrix coordinate system, the both inner and outer boundary conditions are imposed as no-flow boundary, thus the well term is absent in Eq. 3.14. The matrix system only plays as an additional source to the fracture system driven by the differential pressure between fracture and matrix blocks.

3.5.2 Dual Porosity Model Simulation using Fast Marching Method

Zhang et al. (2013) proposed a diffusive time of flight (DTOF) based numerical simulation associated with the transformation of a fluid transport coordinate from the physical 3-D space to the 1-D DTOF space. As in the Convective Time of Flight

(CTOF) applied to the streamline simulation, the DTOF embodies geological heterogeneities and reduces 3-D heterogeneity to a 1-D homogeneous problem along its coordinate. This dimension reduction results in substantial savings in computational time and allows for high resolution reservoir simulation.

Yusuke (2014) extended this DTOF formulation to the dual porosity modeling for single-phase fluid flow problems. The additional coordinate, which is matrix system in dual porosity model, is added to the 1-D fracture system under following assumptions:

(a) The FMM calculation only involves the fracture coordinate system. This means that the FMM calculates the front of the pressure propagation based on the fracture heterogeneities (k_f and ϕ_f).

(b) For simplifying assumption, the matrix properties (i.e. matrix porosity, permeability, shape factor) are assumed to be homogeneous and isotropic, because the geological heterogeneities of the matrix system are not accounted for the DTOF

(c) These treatments will be valid when the fracture network is the system in which the pressure front primarily propagates through and when the matrix serves only as fluid source to the fracture system.

In our research, we followed these assumptions using fast marching method. Fig. 3.6 shows the illustration of the schematic of the DTOF-based dual-porosity model on the 1-D DTOF coordinate.

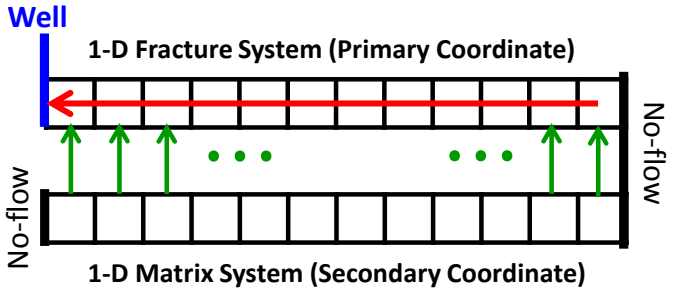

Fig. 3.6 Dual-porosity model on the 1-D DTOF coordinate. (Yusuke 2014)

3.5.3 Dynamic Measure for Dual Porosity Model

In the previous section, dynamic measure for green field using fast marching method (DM_FMM) is defined as the rank normalization of permeability, pore volume and diffusive time of flight obtained from fast marching method.

Unlike single porosity models we dealt with in previous section, dual porosity model has two system, fracture and matrix system, and there are transfers between fracture network and matrix blocks. This transfer function in single phase is expressed as follows:

$$q_{mf} = \sigma \frac{\bar{\rho} k_m}{\mu} \left(\bar{p}_m - p_f \right) \tag{3.15}$$

As we reviewed in prior section, we followed the assumption that matrix properties (i.e. matrix porosity, permeability, shape factor) are homogeneous and isotropic. Therefore, the difference between matrix pressure and fracture pressure became our main concern in this research.

We incorporated the transfer term between fracture network and matrix blocks by adding pressure difference ($p_m - p_f$), to DM_FMM. So, the dynamic measure for dual porosity model using fast marching method (DM_DP) is expressed as follows,

$$Dynamic\,Measure(DM\_DP) = (DTOF_{RN} \cdot \Delta P_{mf_{RN}} \cdot PoreVolume_{RN} \cdot k_{RN}) \quad (3.16)$$

where, ΔP_{mf} is the pressure difference between matrix and fracture.

3.5.4 Dual Porosity Model Case

We applied the new dynamic measure (Eq. 3.9) to dual porosity model. We demonstrated the naturally fractured gas reservoir with one initial vertical well (Fig 3.7(a)). The dimension of this model is 50 by 50 by 5 and the existing producer is at the center of the reservoir.

Fig. 3.7 shows the distribution of matrix permeability and fracture permeability of dual porosity model. Each grid cell is depicted as a sugar cube composed two distinctive domains (Fig.3.7 (b)). The domain at center represents matrix system and the remaining part of the cell surrounding center cube depicts fracture system. According to our assumption, the matrix permeability is set as constant (1×10^{-4} md) and the matrix porosity is also homogeneous (0.1).

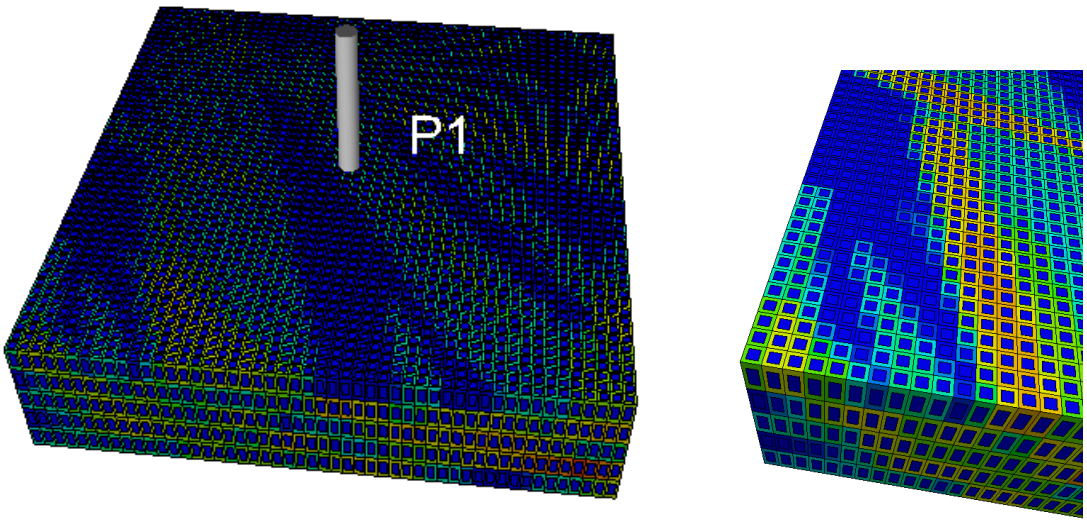

(a) (b)

Fig. 3.7 (a) Sugar Cube Display of Permeability Distribution; (b) Left Lower section view

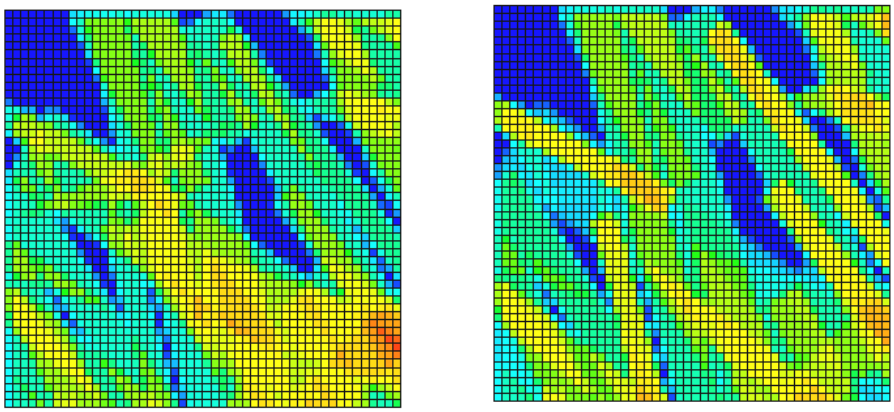

(a) Permeablilty I (b) Permemalibity Z

Fig. 3.8 Distribution of Fracture permeability of Layer 3

According to our new dynamic measure for dual porosity model (DM_DP), we generated dynamic measure map (Fig. 3.9).

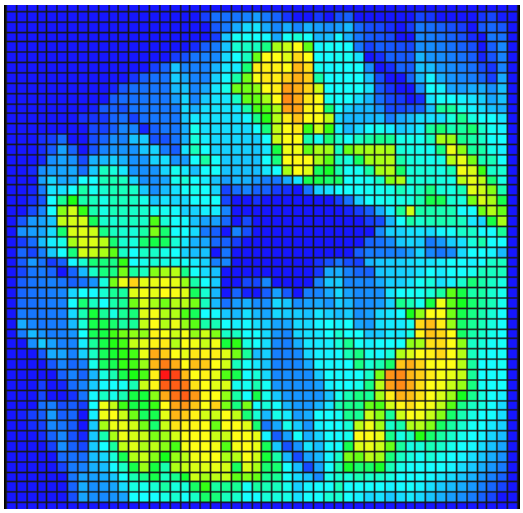

Fig. 3.9 Dynamic Measure Map

As shown in Fig. 3.9, the possible candidate locations can be largely grouped in three regions. We can expect to find optimal well location close to these areas. Fig 3. 10 shows how transfer term affects dynamic measure. Without transfer term, dynamic measure shows higher values around boundaries (Fig. 3.10 (b)). By adding transfer term, which is the pressure difference between fracture network and matrix blocks, the region with higher dynamic measure value shift a little toward the center.

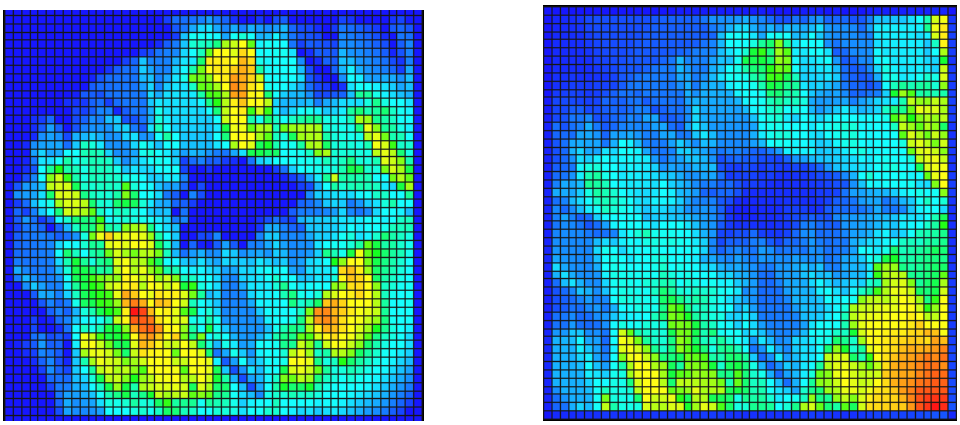

(a) (b)

Fig. 3.10 Dynamic measure (a) with transfer term; (b) without transfer term

To validate our dynamic measure for dual porosity model, we simulated for all possible well locations of candidate well with commercial simulation software. The total gas production for candidate well from is shown in Fig. 3.11 (b). The overall trends are very similar each other and the candidate optimal regions (red and yellowish area) in dynamic measure probability map shows good match with the regions showing high gas production in Fig. 3.11(b).

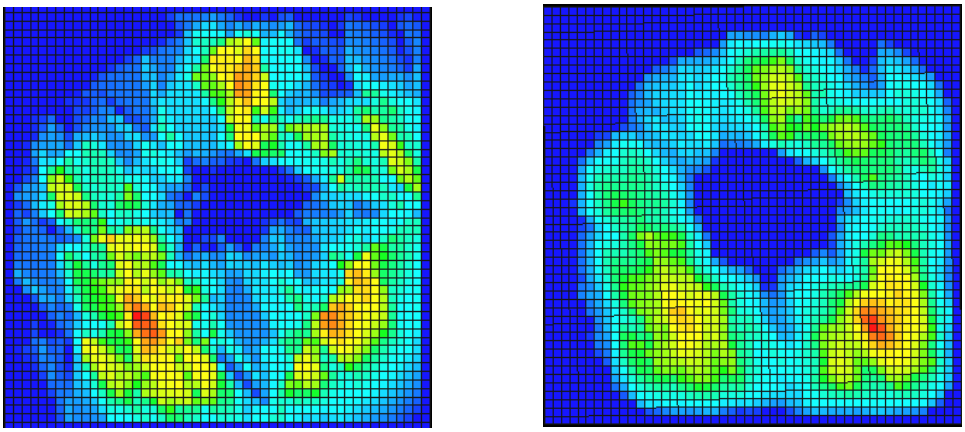

(a) (b)

Fig. 3.11 Comparison of (a) Dynamic Measure (b) Exhaustive Simulation

The following figure shows how genetic algorithm converges to the optimal well location. As expected, hybrid sampling is more efficient to converge to global optimal solution.

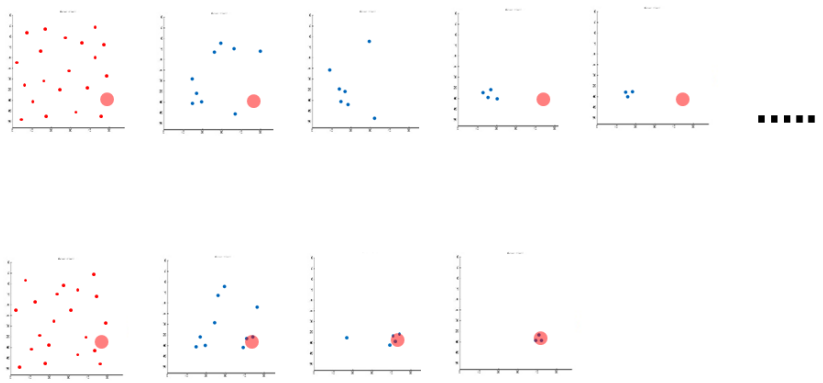

Fig. 3.12 An example of results from (a) random sampling and (b) hybrid sampling

3.6 Summary and Conclusions

In this chapter, we proposed new dynamic measure for primary depletion reservoir. For primary depletion reservoir, we introduced diffusive time of flight term instead of the convective time of flight term used in waterflooding. Diffusive time of flight is a direct analogue for diffusive process of convective time of flight, which provides the underlying technology for streamlines.

Fast marching method (FMM) is used to calculate the diffusive time of flight (DTOF). Starting from asymptotic expansion of the diffusivity equation, we can obtain the propagation of the pressure front for heterogeneous reservoirs, which is in the form of Eikonal equation. This Eikonal equation is solved efficiently by applying FMM. This algorithm provides DTOF values from the source in every grid cells.

The new dynamic measure which is composed of permeability, pore volume and DTOF shows good correlation with exhaustive simulation results. As we showed in previous chapter, better initial candidate locations for constructing response surface for genetic algorithm give faster convergence to the global optimal solution with fewer number of simulations.

We extended the dynamic measure using fast marching method to dual porosity model. In dual porosity model, flow is assumed to be along the fracture network and also between matrix system and fracture system. Therefore, we considered the transfer between matrix and fracture in addition to the flow in the fracture network. For dual porosity model, we were able to take advantage of 1-D DTOF coordinate. Consequently,

we reduce computational expenses not only from hybrid sampling technique but also from fast marching method associated with 1-D DTOF coordinate.

CHAPTER IV

RESERVOIR CHARACTERIZATION USING A STRUCTURED HISTORY MATCHING TECHNIQUE

4.1 Introduction

Understanding the proper geologic characteristics in the reservoir is one of the key aspects of reservoir management, especially in terms of the water flood optimization or the infill location determination. However, in the field with geological complexity, detailed reservoir characterization will be quite challenging because the reservoir fluid dynamics are composite responses of the heterogeneous geologic features and the field operations.

A structured history matching approach which consists of global calibration and local calibration is used for this study. For the global calibration, development of multiple models which match the field performance is our goal. Key global parameters which heavily affects the model response like bottom-hole pressure are selected through a sensitivity analysis. Design of experiments and response surface methodology with evolutionary algorithms such as genetic algorithm are used to calibrate these key global parameters. Then, local calibration using streamline based sensitivity and generalized travel time inversion technique are performed. We utilize streamline-derived analytic sensitivities to determine the spatial distribution and magnitude of the local permeability changes.

4.2 Background

We review the optimization methods for history matching in this section and explain the workflow of streamline-based generalized travel time inversion (GTTI) technique as well as response surface methodology.

4.2.1 History Matching Overview

Calibrating reservoir models to match the history data is essential to predict future reservoir behavior with confidence. Also, it is important to perform computer experiments on methods of managing the reservoir (Oliver and Chen 2011). By calibrating the reservoir models, we intend to adjust the values of the model parameters so that the mathematical model of the reservoir can reproduce the observed behavior as close as possible. It generally involves an inverse problem, which is a history matching process.

In manual history matching, a structured approach is widely used where the sequence of scales of adjustments has been from global, then to flow units which is regional, followed by local changes in model parameters (Cheng et al. 2008). The quality of manual history matching result largely depends on the experience of the reservoir engineers. For large fields, this process becomes very hard to investigate relationships between the model responses and variations of different reservoir parameters.

There have been marked progresses in the ability to generate simulation models to match large amounts of production data by assisted history matching methods in the

last several decades. It is basically similar to manual history matching, except computers and software tools are employed to adjust the reservoir parameters rather than direct intervention of reservoir engineers. Assisted history matching can be treated as a minimization problem, whose objective generally includes a predefined data misfit function and penalty terms to match the observed response. There are several approaches to such minimizations (Yang and Watson 1987; Bissell et al. 1992; Reynolds et al. 1996; Oliver et al. 1997; Datta-Gupta et al. 2001; Cheng et al. 2008) and they can be broadly classified into three categories: gradient-based, sensitivity-based, and derivative-free or direct search methods, respectively.

The gradient-based methods, such as Gauss-Newton method, are intuitive as long as a mathematical minimization of the objective function is well defined. But they generally converge slowly (Bissell et al. 1992) and easy to lead to the nearest local minimum from the starting point instead of the global minimum (Williams et al. 2004; Landa et al. 2005).

Sensitivity-based methods, such as LSQR, have drawn attention due to their faster convergence compared to the gradient-based methods. However, it can be computationally expensive to calculate sensitivity coefficients, which are the partial derivatives of the production response with respect to the reservoir parameters of interest.

The streamline-based generalized travel time inversion (GTTI) technique has proven to be an effective method for calculating the parameter sensitivities (Datta-Gupta et al. 2001; Cheng et al. 2005). It can analytically compute the parameter sensitivities

involving 1D integration along streamlines, which can be generated from either a streamline or a finite-difference simulator.

However, most of deterministic approaches mentioned above generally start with a single initial geological model so that they strongly depend on quality of the initial model. There have been many cases of misrepresentation of large-scale features such as fault communications and pore volumes resulting in unphysical model updates in fine scale reservoir permeability. This is due to the local search nature of the deterministic technique and its deficiency in handling various scale uncertainties. In contrast, global search algorithms avoid the problem of convergence to local optimum nearest to the initial starting point (Cheng et al. 2008) and are able to reconcile multi-scale uncertainties simultaneously. Global search techniques such as simulated annealing (SA) (Galassi 2009; Ouenes and Bhagavan 1994), Markov chain Monte Carlo (MCMC) (Ma et al. 2006; Sambridge 2002) and genetic algorithms (GA) (Holland 1992) have been known to be effective for history matching problems. The advantage of these stochastic search techniques is that they require neither complicated differential equations nor a smooth response space. The primary challenge is that they require large number of flow simulations, which can be computationally prohibitive when the parameter space is very large. Consequently, sensitivity analysis is introduced to rank the importance of model parameters and screen insignificant ones, and the proxy model is introduced as a surrogate to avoid simulations for less likely model candidates (Cheng et al. 2008; Pan and Horne 1998; White and Royer 2003; Yeten et al. 2005; Yeten et al. 2002).

4.2.2 Genetic Algorithm with Proxy Modeling for History Matching

We have applied experimental design and response surface methodologies with evolutionary algorithm for calibration of parameters and to history match production data. The workflow for assisted history matching using proxy and Genetic Algorithm (GA) is similar to the one used in Chapter II. A set of key parameters are selected by sensitivity analysis. The objective functions with respect to selected key parameters are used to generate a response surface proxy using experimental design and response surface methodology. The proxy model is constructed to filter the model whose objective function is higher than unacceptable threshold without running the actual simulation. The evolution is initialized from a set of randomly generated potential individuals. In each generation, the objective function of each individual in the population is evaluated with proxy check. Individuals are randomly selected from current population and modified via GA operators (selection, crossover and mutation) to generate a new population for next iteration. The iteration stops when the maximum number of generations has been reached or satisfactory solution has been achieved.

4.2.3 Streamline-Based Generalized Travel Time Inversion (GTTI)

The goal of GTTI is to calibrate geological model parameter such as permeability or porosity distributions to historical dynamic data. The complete GTTI approach workflow is outlined in Figure 4.1.

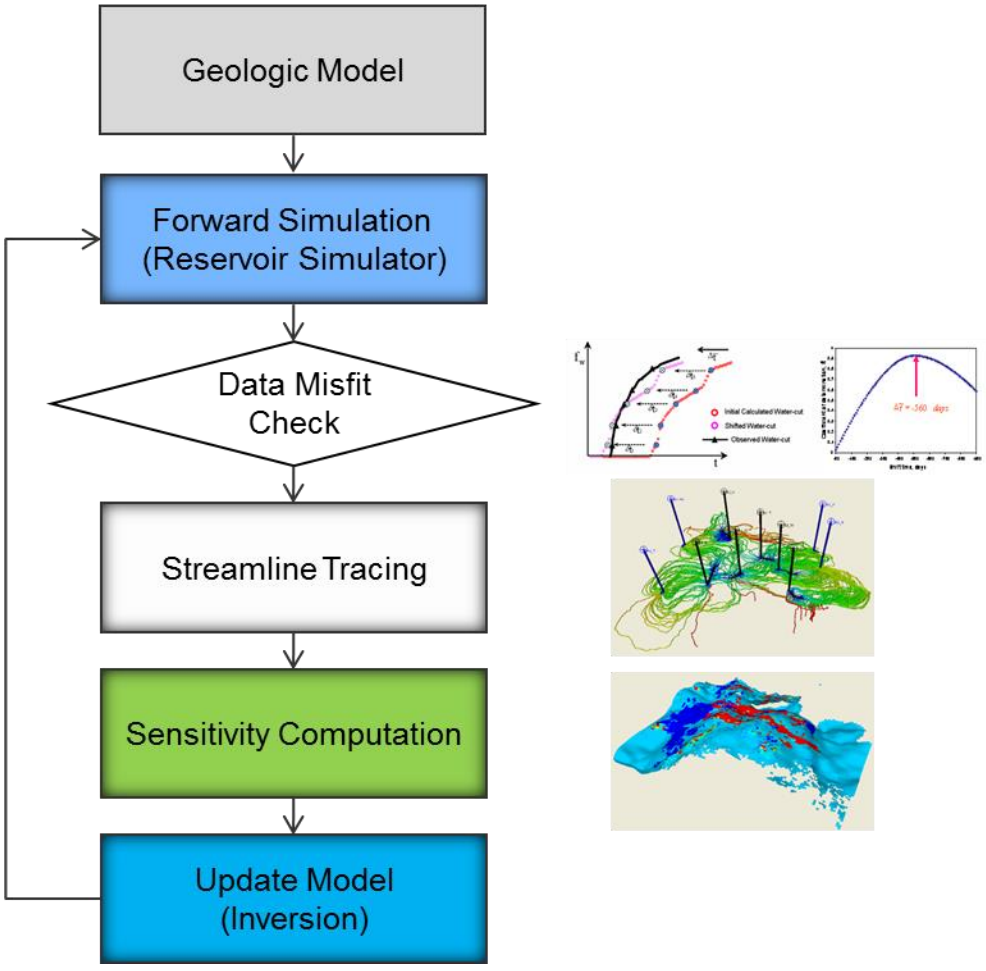

Fig. 4.1 History matching work flow using GTTI

For this kind of inversion problem, the following penalized misfit function is minimized:

$$\|\delta\mathbf{d} - \mathbf{S}\delta\mathbf{R}\| + \beta_1\|\delta\mathbf{R}\| + \beta_2\|\mathbf{L}\delta\mathbf{R}\| \tag{4.1}$$

In the above expression, $\delta\mathbf{d}$ is the data residual vector. It quantifies the difference between the observed and calculated production response and will be expressed by GTT

as discussed later. **S** is the sensitivity matrix that accounts for the change in production response because of a small perturbation in reservoir properties such as permeability or porosity. In other words, sensitivity is simply the partial derivative of production response such as the water front arrival time with respect to the permeability of each grid cell. Also, $\delta\mathbf{R}$ corresponds to the change in the reservoir property and it will be solution of this inversion problem. **L** is a second spatial difference operator. The first term is called the 'data misfit' term that minimizes the difference between the observed and calculated production response. History matching approach can be diverse according to this data. In this project, data misfit is represented by GTT of water-cut profile at the individual well. The second term, 'norm constraint' ensures that the final model is not significantly different from the initial model. This is justified because our initial or prior model already contains sufficient geological and static information related to the reservoir. Finally, the third term, 'roughness penalty' simply recognizes the fact that production data are an integrated response and are, thus, best suited to resolve large-scale structures rather than small-scale property variation. In order to carry out history matching project, data misfit and sensitivity matrix are integral information and thus they need to be computed. GTTI consists of following steps.

4.2.3.1 Computation of Data Misfit

Data misfit is expressed by a GTT at each producing well. GTT is computed by systematically shifting the computed production response toward the observed data until the cross correlation between the two production profiles is minimized. By defining GTT,

we effectively reduce the data mismatch at a well into a single travel-time shift. We are also able to retain many of the desirable properties of travel-time inversion such as a quasi-linear relationship between production response and model parameters. This is explained more in detail in Appendix A.

4.2.3.2 Streamline-Based Sensitivity Computations

Streamline trajectories can be acquired directly from the streamline simulator or can be calculated from the fluid fluxes obtained from the finite-difference simulator with time of flight. Streamlines can account for complex geometry and faulted systems such as non-neighbor connection. The time of flight is then used to compute the sensitivity of GTT with respect to reservoir model parameters. Note that the sensitivity computations require a single flow simulation regardless of the number of parameters. This is explained in detail in Appendix A.

4.2.3.3 Reservoir Model Updating by GTT

This step involves computing the changes in the model parameters by minimizing Eq.(4.1) with a least-squares minimization technique that uses the streamline-derived sensitivity coefficients. Additional constraints are imposed to penalize deviation from a prior or initial model to preserve geologic realism and to restrict permeability changes to large-scale trends consistent with the low resolution of the production data.

4.3 Approach

The history matching process for this research consists of two major steps. First, reservoir energy balance is checked field wide by the given bottom hole pressure data. Second, the well production data are matched using streamline based Generalized Travel Time Inversion (GTTI) technique by modifying local permeability near the wells.

In the global calibration, we use design of experiments and with response surface. The global calibration workflow follows the steps outlined by Schulze-Riegert et al. (2002), Cheng et al. (2008), Yin et al. (2010) and Yin et al. (2011). The global objective function is defined as the sum of logarithms of multiple misfits between simulated and observed data which quantify reservoir energy and flow at a global level, such as field total fluid productions (total liquids, total water, and total gas), well shut-in bottom hole pressures (SBHP). The outcome of the global calibration is an ensemble of plausible geological models matched to the reservoir energy and large scale connectivity.

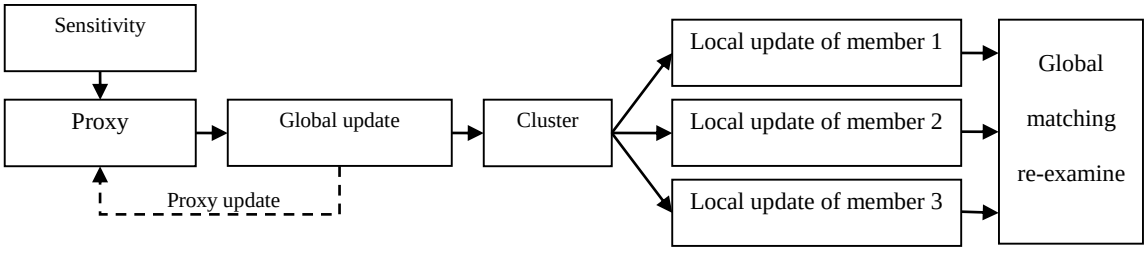

Fig. 4.2 Overview of hierarchical history matching (Yin et al. 2011)

The global updates are followed by local calibration where local parameter sensitivities are used to match water-cut development and well by well response.

Specifically, grid-scale permeability will be adjusted for each ensemble member of the global match in order to match the water-cut, gas-oil-ratio and flowing bottom-hole pressure.

4.4 Geologic Model

The field data have been provided by an oil and gas company for the purpose of research and education. Citations of information from field related literature are not offered for the sake of confidentiality.

The field is producing oil from Miocene reservoirs. Our main interest is in the deeper reservoir of the two Miocene reservoirs. This reservoir is characterized as sand-field channels and overbank deposits in the combination of structural and stratigraphic traps. A major west-east fault dipping to the north and stratigraphic pinch out is in the northeastern and eastern parts. The oil-water contact (OWC) of the main part of the reservoir is estimated at 14,300 ft according to literature review.

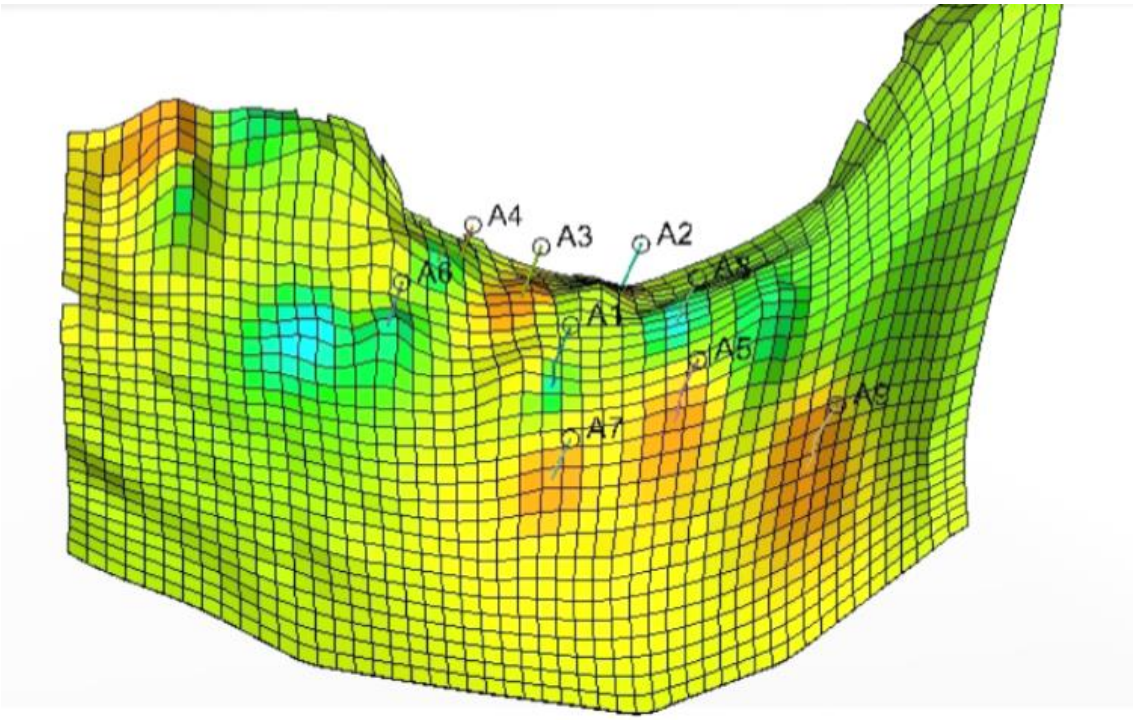

Fig. 4.3 The structure of the reservoir

There are 7 producers and 2 water injectors in this reservoir model. Our geological model has 50 by 30 by 20 dimension and there are 7 geological regions which are divided according to seismic amplitude difference in 6 years. If we have dimming seismic amplitude, we can attribute it to increasing water saturation. Therefore, the amplitude outline gives a good indication of the extent of the sand in north-south direction.

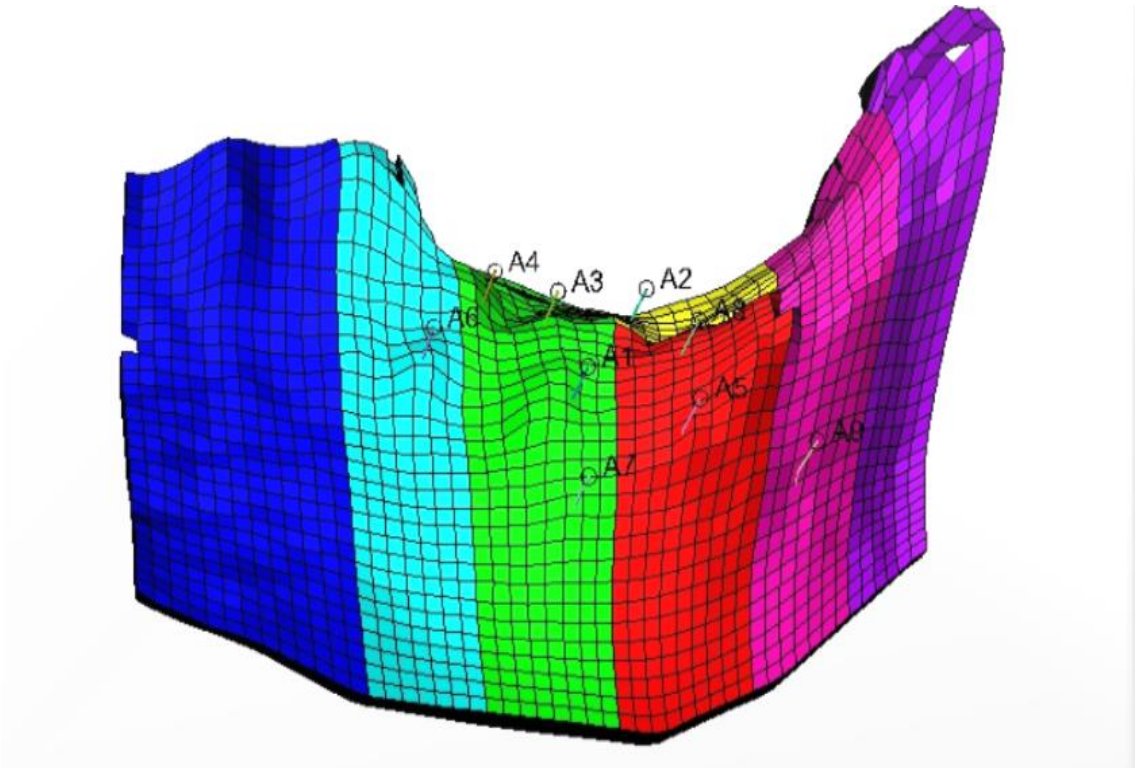

Fig. 4.4 Seven geological regions by seismic amplitude change

After literature review of turbidite reservoir characterization, multiple geologic models were generated by three chosen criteria, architecture, net sand thickness and connectivity. We built low, mid and high cases for each criterion. For example, low amalgamated, mid amalgamated and high amalgamated models were generated for the criterion of architecture. Each of the 27 geologic models was calibrated using proxy GA to condition well data including shut-in bottom-hole pressures and cumulative liquid productions. Each updated ensemble of geologic model realization provides an estimation of STOIIP. Specifically, for each geologic model, regional and inter-regional uncertainties were introduced and analyzed including pore volume multipliers and

horizontal permeability multipliers, and aquifer strength. Table 4.1 shows the final list of key global variables for GA after sensitivity analysis of a selected geologic model, and the right column shows a realization of updated multipliers.

Table 4.1 List of key global variables and their ranges from sensitivity analysis

Variable Multiplier	**Min**	**Max**	**Result**
PERMX3	0.1	1.0	0.497
PERMX5	0.1	2.0	0.521
PERMX6	0.1	1.0	0.232
Kv/Kh	0.05	1.0	0.191
PORV2	0.1	1.0	0.389
PORV5	0.1	1.5	0.595
AQUIFER	100	500	172

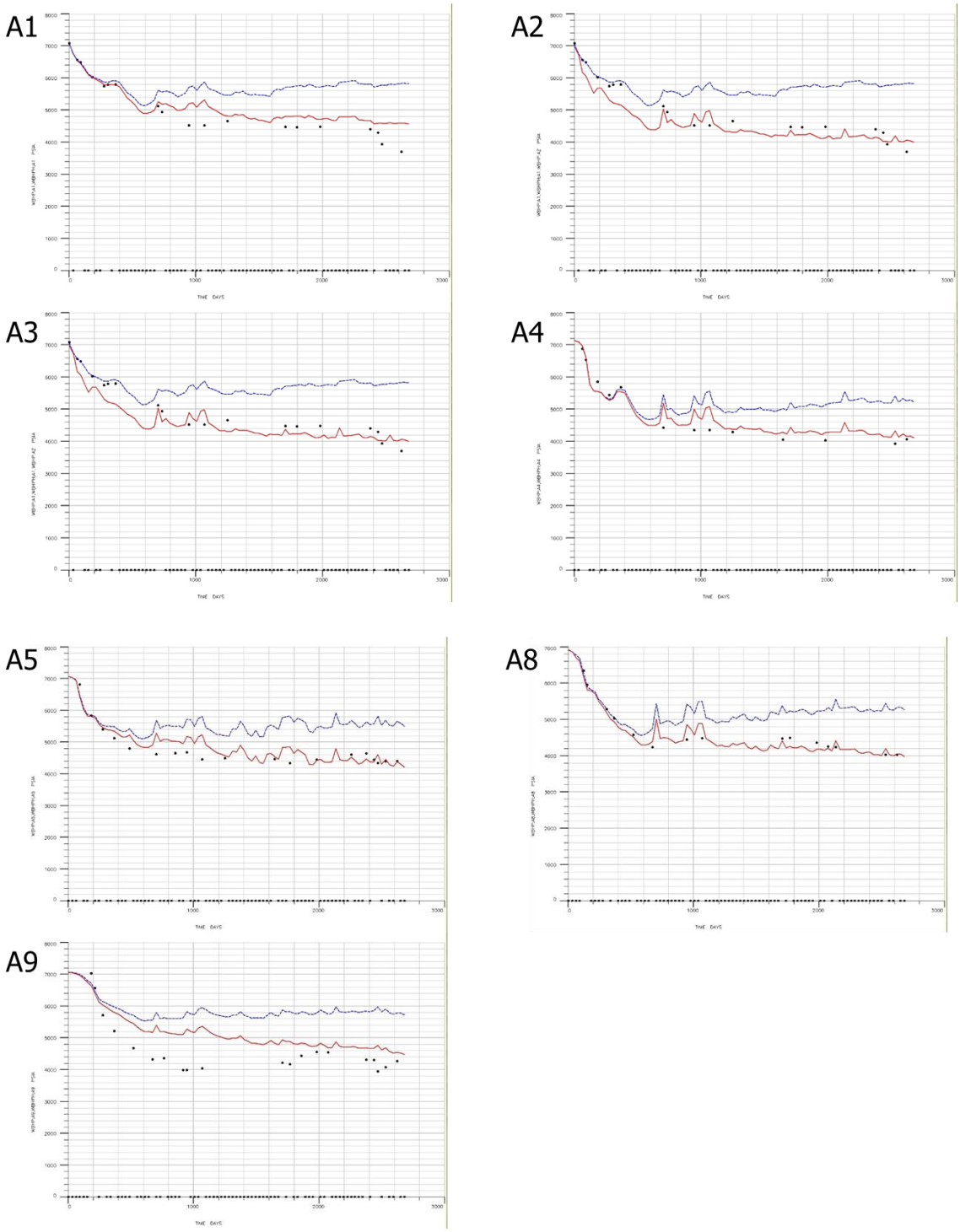

Fig. 4.5 Global pressure match

4.5 Simulation Results

4.5.1 Global Pressure Match

Fig. 4.5 shows the well bottom hole pressure match for one selected geologic model after global update. Black dots are actual history data of bottom-hole pressure, blue lines represents the bottom-hole pressure of initial model and red lines are updated bottom-hole pressure after global match. The overall pressure has been lowered after we updated global parameters. We checked the adjusted simulation model with actual data. The overall pressure match has been improved.

4.5.2 Local Saturation Match

The well-level history matching results are shown in Figure 4.6. Let's discuss the history matching procedures with well A2 results in this figure. GTTI investigates the water front movement and its arrival time via the well water cut profile. In Figure 4.6, the initial simulation model results (blue dashed line) show the earlier water breakthrough and consequently has less oil production than the field history. In order to mitigate this time discrepancy, GTTI defines the sensitivity coefficient using streamline trajectories. With streamline trajectories, we can easily define the effective region for the water production of a well and also can compute the sensitivity value analytically. Then, connectivity or permeability between the producer, A2, and injectors nearby or water influx are updated based on the data misfit. In the A2 case, the permeability around CM109 decreased to move the water front arrival backward. The oil production rate match concurrently improved as a result of the water cut matching.

Basically, the GTTI considers the water breakthrough time in the water cut profile as data for the history match. However, often the water cut mismatch between production history and the simulation results is not due to the connectivity between the producer and injectors. Other reasons such as locally low reservoir pressure or a small productivity index may cause the water cut misfit. If we modify the well connectivity carelessly in those cases, the reservoir characterization may deteriorate.

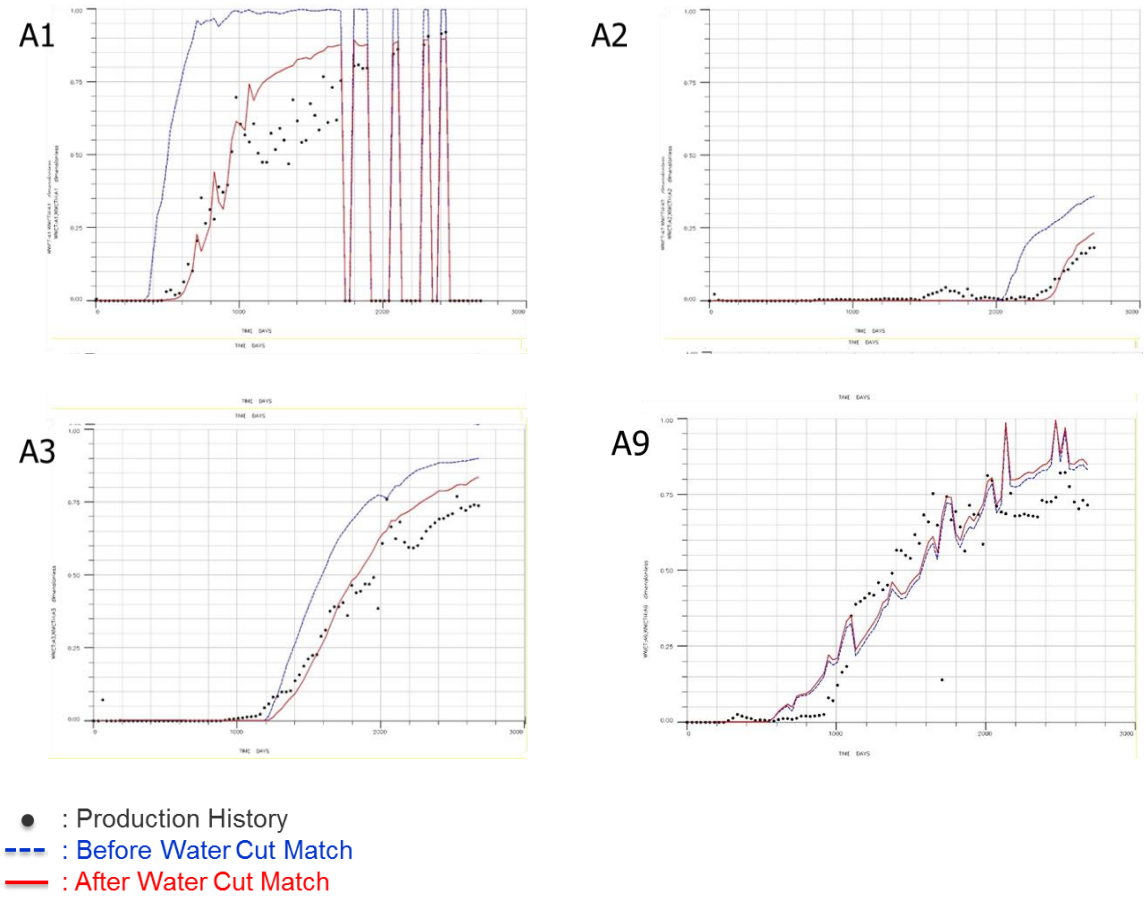

Fig. 4.6 Local saturation match (Well water cut)

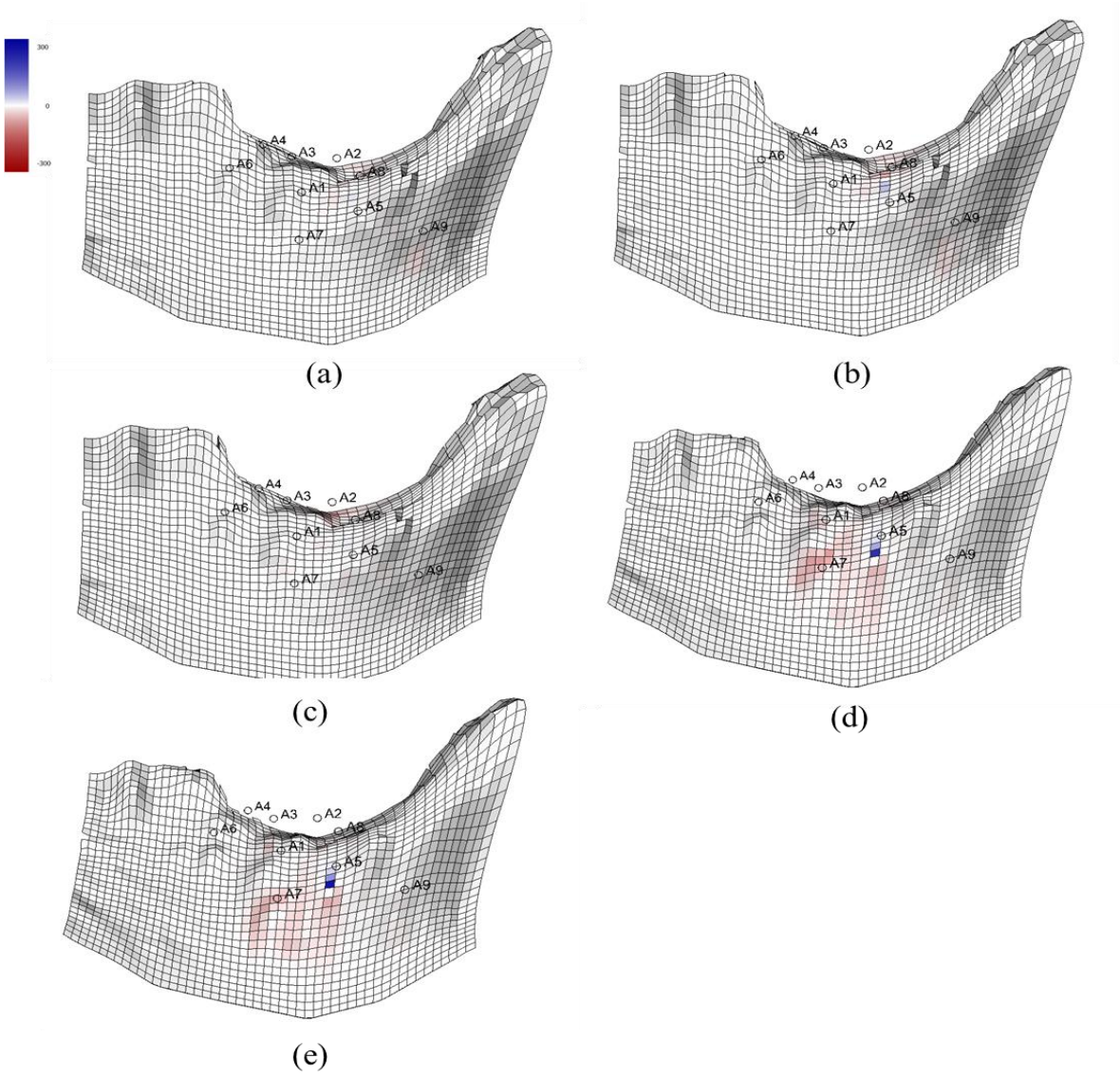

Fig. 4.7 Permeability change after local update (a) layer 4, (b) layer 5, (c) layer 7, (d) layer 14, (e) layer 15

Fig. 4.7 shows the permeability changes in several layers through the local saturation updates. Red color represents that permeability has been decreased via updates, whereas blue color shows permeability has been increased during the updates. Overall, red color dominates blue color throughout the layers. It means our connectivity

level may be higher than actual field data. The red colors are around A7 and between A5 and A7. It means the transmissibility between A7 and A5 are lower than our initial geologic model. It might be the evidence that the channels are not as much amalgamated with each other as we originally thought. However, if we start from a different geological realization with less amalgamated model, the permeability changes would be different and we may see increased transmissibility probably between the producing wells through the updates. We need to be more cautious when we select the parameters and analyze how they are sensitive to our objective function.

4.6 Summary and Conclusions

In this chapter, we presented a workflow of structured history matching approach and applied it to a turbidite reservoir. The hierarchical workflow composed of global and local calibration will provide a useful tool for reservoir characterization.

A hybrid stochastic approach based on the genetic algorithm combined with a proxy model for the objective function more effectively finds preliminary solutions for global parameters by matching pressure response. Then, solutions acquired from global calibration are used for the local updates.

Streamline-based sensitivity and Generalized Travel Time Inversion (GTTI) algorithms are used for local calibration. Streamline-derived analytic sensitivities are used to determine and update distribution and magnitude of permeability near wells. With the reservoir energy level calibrated from global updates, the GTTI technique finds solutions very quickly for global updated models.

Within the GTTI algorithms, the local permeability changes are regularized by the term of nom constraint such that the final model is not significantly different from the globally updated models. Therefore, we can match the local distribution while keeping the global energy level.

CHAPTER V

CONCLUSIONS AND RECOMMENDATIONS

5.1 Conclusions

In this work, we have presented the applications of hybrid optimization methods to the problems of field development. During the field development, finding optimal well locations and prediction of the reservoir responses are very crucial to make the project successful one. Reliable models obtained through the history matching processes helps to understand how the reservoir performance will be and to select optimal well location plan for the future development.

First, we proposed the workflow of a hybrid sampling method associated with genetic algorithm and applied it to waterflooding field case. The response surface methodology combined with dynamic measure sampling technique provides the proxy model for the genetic algorithm. Also, we combined initial candidate well locations sampled from design of experiments for the purpose of exploring the regions dynamic measure sampling might miss.

Second, we presented a new dynamic measure for fields under primary depletion. Instead of the convective time of flight term used for the waterflooding field case, we introduced the diffusive time of flight term calculated from the fast marching method. Diffusive time of flight is a direct analogue for diffusive processes of convective time of flight, which provides the underlying technology for streamlines. We also extended our approach to the dual porosity model. In dual porosity model, flow is assumed to be along

the fracture network and between matrix and fracture. Therefore, we added the transfer term between matrix and fracture to dynamic measure to incorporate the inter-porosity flow.

Third, a structured history matching approach which consists of global calibration and local calibration was presented. Key global parameters which heavily affect the model responses are selected through a sensitivity analysis. Design of experiments and response surface methodology with evolutionary algorithms such as genetic algorithm are used to calibrate these key global parameters. Then, local calibration using streamline based sensitivity and generalized travel time inversion technique are performed. We utilize streamline-derived analytic sensitivities to determine the spatial distribution and magnitude of the local permeability changes.

In conclusion, dynamic measure, an indicator of remaining oil in the reservoir, is consolidated with the hybrid sampling method and used as a proxy model for the well placement optimization. Genetic algorithm proved to be a good tool for the well placement optimization since it avoids trapping in local minima. Proxy model sampled from dynamic measure probability map enabled genetic algorithm to converge to optimal solution with fewer evaluation. Hybrid sampling method is a combined sampling technique composed of dynamic measure sampling and random sampling. Randomly sampled candidate well locations can cover the region dynamic measure sampling might miss. Hybrid sampling method proved to be more efficient than dynamic measure sampling.

For primary depletion reservoir, the new dynamic measure which is composed of permeability, pore volume and DTOF showed good correlation with exhaustive simulation results. As we shown in the chapter II, better initial candidate locations for genetic algorithm give convergence to the global optimal solution with fewer number of simulations. Also, we extended dynamic measure using fast marching method to dual porosity model. By considering the transfer between matrix and fracture in addition to the flow in the fracture network, we obtained better correlation. For dual porosity model, we were able to take advantage of 1-D DTOF coordinate. Consequently, we reduced computational expenses not only from hybrid sampling technique but also from fast marching method associated 1-D DTOF coordinate.

The hierarchical workflow composed of global and local calibration has several advantages. First, a hybrid stochastic approach based on the genetic algorithm combined with a proxy model for the objective function more effectively finds preliminary solutions to match global parameters like bottom-hole pressure. Second, streamline-derived analytic sensitivities are used to determine and update distribution and magnitude of permeability near wells. With the reservoir energy level calibrated from global updates, this GTTI technique finds solutions very quickly for global updated models. Third, within the GTTI algorithms, the local permeability changes are regularized by the term of nom constraint such that the final model is not significantly different from the globally updated models. Therefore, we can match the local distribution while keeping the global energy level.

5.2 Future Work and Recommendations

In our study, genetic algorithm (GA) is used to establish workflows to accomplish model calibration and data integration. For hybrid stochastic methods, there are some other stochastic algorithms such as Particle Swarm Optimization (PSO) used for optimization problems in field development. We may try which optimization methods will be more suitable for each kind of optimization. If we find more suitable algorithm for a specific optimization, we will find solutions more efficiently. Even with genetic algorithm, we may find better set of GA operators through sensitivity analysis.

In this work, we assumed a vertical well for the well placement optimization problems. Our work can be applied to conventional type of wells. However, it is necessary to extend our work to non-conventional type well problems. More studies about well types and well patterns will be needed to solve the optimization problems for non-conventional wells which have now become very common.

The proposed dynamic measure in Chapter III is applied to single phase reservoir. It can be extended to multi-phase reservoir with the advent of more elaborate application of fast marching method.

For dual porosity model, we can further explore the effect of other parameters which can affect the flow rate, such as interporosity flow coefficient and storativity ratio. The effect of these two terms doesn't appear significant in our study. However, if we apply this method to different types of reservoir, such as extremely tight reservoir, the effect might be significant.

REFERENCES

Artus, V., Durlofsky, L.J., Onwunalu, J., and Aziz, K. 2006. Optimization of Nonconventional Wells under Uncertainty Using Statistical Proxies. *Computational Geosciences* **10** (4): 389-404.

Bissell, R., Killough, J.E., and Sharma, Y. 1992. Reservoir History Matching Using the Method of Gradients on a Workstation. SPE 24265-MS.

Bittencourt, A. and Horne, R. 1997. Reservoir Development and Design Optimization. Paper SPE 38895 presented at the SPE Annual Technical Conference and Exhibition, San Antonio, Texas, USA.

Blair, P.M. 1964. Calculation of Oil Displacement by Countercurrent Water Imbibition. *Society of Petroleum Engineers Journal* **4** (3): 195-202.

Cheng, H., Datta-Gupta, A., and He, Zhong. 2005. A Comparison of Travel Time and Amplitude Inversion for Production Data Integration into Geologic Models: Sensitivity, Non-linearity and Practical Implications. *Society of Petroleum Engineers Journal* **10** (1): 75-90.

Cheng, H., Dehghani, K., and Billiter, T.C. 2008. A Structured Approach for Probabilistic-Assisted History Matching Using Evolutionary Algorithms: Tengiz Field Applications. SPE 116212-MS.

Da Cruz, P.S., Horne, R.N., and Deutsch, C.V. 2004. The Quality Map: A Tool for Reservoir Uncertainty Quantification and Decision Making. *SPE Reservoir Evaluation & Engineering* **7** (1): 6–14. SPE 87642-PA.

Dean, R.H., and Lo, L.L. 1988. Simulations of Naturally Fractured Reservoirs. *SPE Reservoir Engineering* **3** (2): 638-648.

Datta-Gupta, A., Kulkarni, K.N., Yoon, S., and Vasco, D.W. 2001. Streamlines, Ray Tracing and Production Tomography: Generalization to Compressible Flow. *Petroleum Geoscience* **7**: 75-86.

Datta-Gupta, A., and King, M.J. 2007. *Streamline Simulation: Theory and Practice*. Textbook Series, Society of Petroleum Engineers, Richardson, Texas, USA.

Datta-Gupta, A., Xie, J., Gupta, N., King, M. J. and Lee W. J. 2011, Radius of Investigation and its Generalization to Unconventional Reservoirs, *Journal of Petroleum Technology*, **63** (7): 52-55.

Emerick, A., Silva, E., Messer, B., Almeida, L., Szwarcman, D., Pacheco, M.A., and Vellasco, M. 2009. Well Placement Optimization Using a Genetic Algorithm with Nonlinear Constraints. Paper SPE 118808 presented at the SPE Reservoir Simulation Symposium, Woodlands, Texas, USA. SPE 118808-MS.

Galassi, M., Davis, J., Theiler, J., Gough, B., Jungman, G. et al. 2009. Gnu Scientific Library Reference Manual: UK: Network Theory Ltd., Original edition. ISBN 0954612078.

Guyaguler, B. 2002. Optimization of Well Placement and Assessment of Uncertainty. Ph.D Thesis.

Guyaguler, B., and Horne, R. 2004. Uncertainty Assessment of Well Placement Optimization. *SPE Reservoir Evaluation & Engineering* **7** (1): 24-32. SPE 87663-PA.

Holland, J.H. 1992. Genetic Algorithms. *Scientific American* **267** (1): 44-50.

Kazemi, H., Merrill, L.S., Porterfield, K.L., and Zeman, P.R. 1976. Numerical Simulation of Water-Oil Flow in Naturally Fractured Reservoir. *Society of Petroleum Engineers Journal* **16** (6): 317-326.

Kazemi, H., and Merrill, L.S. 1979. Numerical Simulation of Water Imbibition in Fractured Cores. *Society of Petroleum Engineers Journal* **19** (3): 175-182.

Kharghoria, A., Cakici, M., Narayanasamy, R., Kalita, R., Sinha, S., and Jalali, Y. 2003. Productivity-Based Method for Selection of Reservoir Drilling Target and Steering Strategy. Paper SPE 85431 presented at the SPE/IADC Middle East Drilling Technology Conference and Exhibition, Abu Dhabi, United Arab Emirates. SPE 85431-MS.

Kim, J. U., Datta-Gupta, A., Brouwer, R. and Haynes, B.Jr. 2009. Calibration of High-Resolution Reservoir Models Using Transient Pressure Data. SPE 124834-MS.

Landa, J. Kalia, P.K., Nakano, A., and Vashishta, P. 2005. History Match and Associated Forecast Uncertainty Analysis—Practical Approaches Using Cluster Computing. Paper IPTC 10751 presented at the SPE Annual Technical Conference and Exhibition, Denver, 5-8 October.

Lee, W.J. 1982. *Well Testing*. SPE Textbook Series. Richardson, Texas, USA.

Liu, N., and Jalali, Y. 2006. Closing the Loop between Reservoir Modeling and Well Placement and Positioning. Paper SPE 98198 presented at the Intelligent Energy Conference and Exhibition, Amsterdam, Netherlands. SPE 98198-MS.

Ma, X., Al-Harbi, M., Datta-Gupta, A. et al. 2006. A Multistage Sampling Method for Rapid Quantification of Uncertainty in History Matching Geological Models. SPE 102476-MS.

Oliver, D.S., Cunha, L.B., Reynolds, A.C. 1997. Markov chain Monte Carlo methods for conditioning a ppermeability field to pressure data. *Math Geol.* **29** (1): 61-91.

Oliver, D.S., Chen, Y. 2011. Recent Progress on Reservoir History Matching: A Review. *Comput Geosci* **15**: 185-221

Ouenes, A. and Bhagavan, S. 1994. Application of Simulated Annealing and Other Global Optimization Methods to Reservoir Description: Myths and Realities. SPE 28415-MS.

Pan, Y. and Horne, R.N. 1998. Improved Methods for Multivariate Optimization of Field Development Scheduling and Well Placement Design. SPE 49055-MS.

Reynolds, A.C., He, N., Chu, L., Oliver, D.S. 1996. Reparameterization techniques for generating reservoir descriptions conditioned to variograms and well-test pressure data. *Society of Petroleum Engineers Journal* **1**(4): 413-426. SPE 30588-PA.

Sambridge, M., Mosegaard, K. 2002. Monto Carlo Methods in Geophysical Inverse Problems. *Reviews of Geophysics* **40** (3): 1009.

Sarma, P., and Chen, W.H. 2008. Efficient Well Placement Optimization with Gradient-Based Algorithms and Adjoint Models. Paper SPE 112257 presented at the SPE Intelligent Energy Conference and Exhibition, Amsterdam, Netherlands. SPE 112257-MS.

Sawyer, S.A.,Parsch, J.,Zhang, Z., and Hartl, D.L. 2007. Prevalence of positive selection among nearly neutral amino acid replacements in Drosophila. *Proceedings of the National Academy of Sciences of the United States of America* **104** (16): 6504-6510.

Schulze-Riegert, R.W., Axmann, J.K., Haase, O., Rian, D.T., and You, Y.L. 2002. Evolutionary Algorithms Applied to History Matching of Complex Reservoirs. *SPE Reservoir Evaluation & Engineering* **5** (2): 163-173. SPE 77301-PA.

Sethian, J. A. 1996. A Fast Marching Level Set Method for Monotonically Advancing Fronts. *Proceedings of the National Academy of Science* **93**: 1591-1595.

Sethian, J. A. 1999. Fast Marching Methods. *SIAM Review* **41**: 199-235.

Taware, S., Park, H., Datta-Gupta, A. et al. 2012. Well Placement Optimization in a Mature Carbonate Waterflood using Streamline-based Quaility Maps. SPE 155055-MS.

Vasco, D.W., Keer, H., and Karasaki, K. 2000. Estimation of Reservoir Properties Using Transient Pressure Data: An Asymptotic Approach. *Water Resources Research* **36** (12): 3447-3465.

Warren, J.E. and Root, P.J. 1963. The Behavior of Naturally Fractured Reservoirs. *Society of Petroleum Engineers Journal* **3** (3): 245-255.

Weise T. 2008. *Global Optimization Algorithms-Theory and Application*. 3: 114. E-book at http://www.it-weise.de/

White, C.D. and Royer, S.A. 2003. Experimental Design as a Framework for Reservoir Studies. SPE 79676-MS.

Williams, G.J.J., Mansfield, M., MacDonald, D.G., and D. Bush 2004. Top-Down Reservoir Modeling. SPE 89974-MS.

Xie, J., Gupta, N., King, M. J., and Datta-Gupta, A. 2012a, Depth of Investigation and Depletion Behavior in Unconventional Reservoir Using Fast Marching Methods, SPE 154532-MS.

Yang, P.H., Watson, A.T.1987. Automatic History-Matching with Variable-Metric Method. SPE 16977-MS.

Yeten, B., Durlofsky, L.J., and Aziz, K. 2002. Optimization of Nonconventional Well Type, Location and Trajectory. SPE 77565-MS.

Yeten, B., Durlofsky, L., and Aziz, K. 2003. Optimization of Nonconventional Well Type, Location and Trajectory. *Society of Petroleum Engineers Journal* **8** (3): 200-10. SPE 86880-PA.

Yeten, B., Castellini, A., Guyaguler, B. et al. 2005. A Comparison Study on Experimental Design and Response Surface Methodologies. SPE 93347-MS.

Yin, J., Park, H., Datta-Gupta, A. et al. 2010. A Hierarchical Streamline-Assisted History Matching Approach with Global and Local Parameter Updates. SPE 132642-MS.

Yin, J., Xie, J., Datta-Gupta, A. and Hill, A.D. 2011. Improved Characterization and Performance Assessment of Shale Gas Wells by Integrating Stimulated Reservoir Volume and Production Data. SPE 148969-MS.

Yusuke F. 2014. Fast Marching Method with Multiphase Flow and Compositional Effects. Master Thesis

Zhang, Y., Yang, C., King, M.J., and Datta-Gupta, A. 2013. Fast-Marching Methods for Complex Grids and Anisotropic Permeabilities: Application to Unconventional Reservoirs. SPE 163637-MS.

APPENDIX A

GENERALIZED TRAVEL TIME INVERSION

GTT and Data Misfit

Geologic model calibration via Generalized Travel Time Inversion (GTTI) requires minimization of the data misfit in

$$\|\delta\mathbf{d} - \mathbf{S}\delta\mathbf{R}\| + \beta_1\|\delta\mathbf{R}\| + \beta_2\|\mathbf{L}\delta\mathbf{R}\| \tag{A.1}$$

As shown in Figure A.1, we systematically shift the simulated WWCT curve and compute the correlation coefficient between the observed WWCT curve and shifted simulated WWCT curve. For instance, suppose that we shift 360 days the original simulation WWCT. The shifted WWCT curve will be located as shown in Figure 1(a), and then correlation coefficient with the observed history is computed. This calculated correlation coefficient consists of one point in Figure 1(b). Similarly we repeat the shifting and correlation coefficient calculation within entire production range. The 'optimal' shifting time, which we call GTT, is given at the maximum correlation coefficient. In the example in Figure 1, GTT is 560 days. In GTTI approach we handle a single data misfit value an individual well. This aspect facilitates a quasi-linear behavior during inversion process more than the case of the amplitude misfit of individual WWCT point. In other words, the relationship between the well production performance given by GTT and reservoir model parameter is more linear than that between individual WWCT point and parameters. This

quasi-linear behavior is a favorable characteristic for inversion process and is encapsulated by sensitivity coefficient of each grid property as discussed in next section.

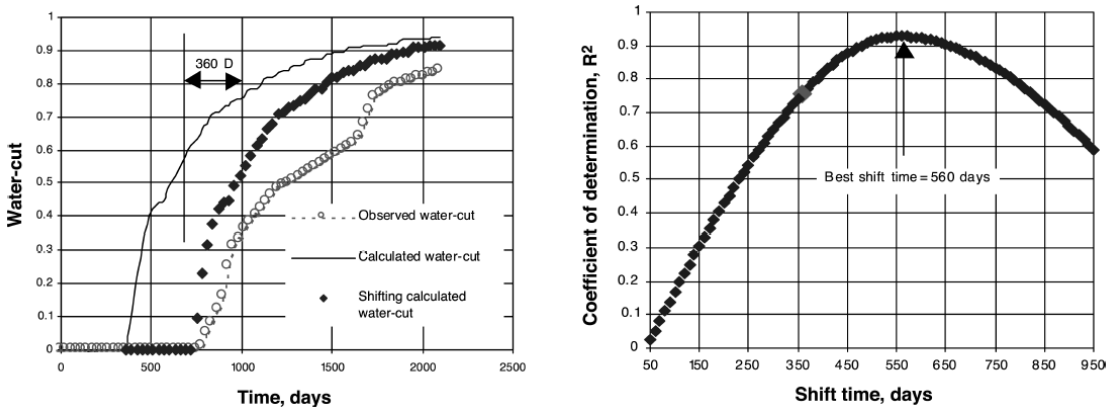

(a) Shifting of WWCT curve (b) Correlation Coefficient

Fig. A.1 Example of Determination of GTT

Streamline-Based Sensitivity Coefficient

Sensitivity Coefficient

Sensitivity is simply the partial derivative of the well production performance which is represented by GTT with respect to the model property of each grid. It is more demonstrative when we review the sensitivity matrix and its component in Eq. A.2

$$\begin{bmatrix} \frac{\partial d_1}{\partial m_1} & \frac{\partial d_1}{\partial m_2} & \cdots & \frac{\partial d_1}{\partial m_M} \\ \frac{\partial d_2}{\partial m_1} & \ddots & & \vdots \\ \vdots & & \ddots & \vdots \\ \frac{\partial d_N}{\partial m_1} & \cdots & \cdots & \frac{\partial d_N}{\partial m_M} \end{bmatrix} \tag{A.2}$$

Where,

N: the number of dynamic data

M: the number of model parameters (i.e. number of permeability (grid block))

d: dynamic data (i.e. GTT of WWCT)

m: model parameter (i.e. permeability)

For instance, d_1 is the GTT of WWCT in well #1, and $\partial d_1/\partial m_2$ is the change of the arrival time of the water front in well #1 resulting from a perturbation in the permeability of grid block #2.

The next basic concept for streamline based formulation is coordinate transformation from physical space to time-of-flight.

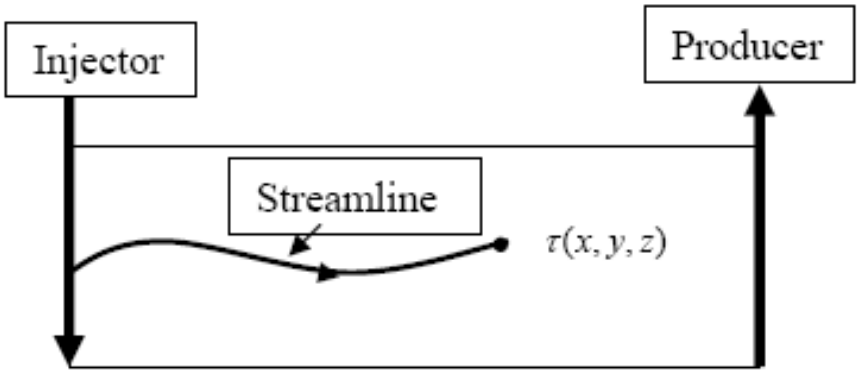

Fig. A.2 Time of Flight as a Coordinate System

Figure A.2 describes the concept of time of flight as a coordinate system. We can locate the position when time of flight is known along specific streamline. This can be expressed by following mathematical formulation:

$$\tau(\mathbf{x}) = \int_{\Psi} \frac{dr}{|\mathbf{v}(\mathbf{x})|}$$

$$\mathbf{v}(\mathbf{x}) \cdot \nabla \tau(\mathbf{x}) = 1 \qquad * \text{ along streamline } \Psi$$

$$\mathbf{v}(\mathbf{x}) \cdot \nabla = \frac{\partial}{\partial \tau} \qquad * \text{ operator identity}$$

, where (A.3)

$\mathbf{v}(\mathbf{x}) = \dfrac{\mathbf{u}(\mathbf{x})}{\phi}$: interstitial velocity

$\tau(\mathbf{x})$: travel time of a neutral tracer along streamline Ψ

dr : distance along streamline Ψ

We can derive the sensitivity of time-of-flight as shown in Eq. A.4

$$\tau(\mathbf{x}) = \int_{\Psi} \frac{dr}{|\mathbf{v}(\mathbf{x})|} = \int_{\Psi} s(\mathbf{x}) dr \qquad * \text{slowness}, s(\mathbf{x})$$

$$s(\mathbf{x}) = \frac{1}{|\mathbf{v}(\mathbf{x})|} = \frac{\phi}{|\mathbf{u}(\mathbf{x})|} = \frac{\phi(\mathbf{x})\mu}{k(\mathbf{x})|\nabla p|}$$

$$\frac{\partial s(\mathbf{x})}{\partial k(\mathbf{x})} = -\frac{\phi(\mathbf{x})\mu}{k(\mathbf{x})^2|\nabla p|} = -\frac{s(\mathbf{x})}{k(\mathbf{x})}$$

$$\frac{\partial s(\mathbf{x})}{\partial \phi(\mathbf{x})} = \frac{\mu}{k(\mathbf{x})|\nabla p|} = \frac{s(\mathbf{x})}{\phi(\mathbf{x})}$$

$$\delta\tau = \int_{\Psi} \delta s(\mathbf{x}) dr = \int_{\Psi} \left[\frac{\partial s(\mathbf{x})}{\partial k(\mathbf{x})} \delta k(\mathbf{x}) + \frac{\partial s(\mathbf{x})}{\partial \phi(\mathbf{x})} \delta \phi(\mathbf{x}) \right] dr$$

$$= \int_{\Psi} \left[-\frac{s(\mathbf{x})}{k(\mathbf{x})} \delta k(\mathbf{x}) + \frac{s(\mathbf{x})}{\phi(\mathbf{x})} \delta \phi(\mathbf{x}) \right] dr \qquad \text{(A.4)}$$

$$\frac{\partial \tau(\Psi)}{\partial k(\mathbf{x})} = \int_{inlet}^{outlet} \left[-\frac{s(\mathbf{x})}{k(\mathbf{x})} \right] dr = -\frac{s(\mathbf{x})}{k(\mathbf{x})} \Delta r = -\frac{\Delta \tau}{k(\mathbf{x})} \qquad * \Delta r : \text{the arc length of the streamline}$$

$$\frac{\partial \tau(\Psi)}{\partial \phi(\mathbf{x})} = \int_{inlet}^{outlet} \left[\frac{s(\mathbf{x})}{\phi(\mathbf{x})} \right] dr = \frac{s(\mathbf{x})}{\phi(\mathbf{x})} \Delta r = \frac{\Delta \tau}{\phi(\mathbf{x})} \qquad \text{within the grid block at } \mathbf{x}$$

Thus, the time of flight sensitivity of a certain grid can be simply computed by the time of flight after streamline tracing since the time of flight is also computed during calculation of the streamline trajectories. This time of flight sensitivity makes a great role in dynamic data integration afterward.

Water-cut Sensitivity

In this section we will review the sensitivity of Well Water Cut (WWCT) in the incompressible case for convenience of derivation. Using incompressibility and the operator identity in Eq. A.5 the continuity equation for the water phase is simplified as follows:

$$
\begin{aligned}
&\phi \frac{\partial S_w}{\partial t} + \nabla \cdot \left(f_w \mathbf{u}_t \right) = 0 \\
&\phi \frac{\partial S_w}{\partial t} + f_w \nabla \cdot \mathbf{u}_t + \mathbf{u}_t \cdot \nabla f_w = 0 \\
&\phi \frac{\partial S_w}{\partial t} + f_w \nabla \cdot \mathbf{u}_t + \phi \frac{\partial f_w}{\partial \tau} = 0 \\
&\frac{\partial S_w}{\partial t} + \frac{\partial f_w}{\partial \tau} = 0
\end{aligned}
\tag{A.5}
$$

Eq. A.5 is the Buckley-Leverett equation for incompressible flow in the time of flight coordinate system. We can rewrite Eq. A.6,

$$
\left. \frac{\partial \tau}{\partial t} \right|_{Sw} = \frac{df_w}{dS_w} \tag{A.6}
$$

The physical meaning of Eq. A.7 is the velocity of a given saturation contour S_w along a streamline. Thus, the arrival time of the saturation front is

$$
t = \tau \Big/ \frac{df_w}{dS_w} \tag{A.7}
$$

Finally, the sensitivity of the saturation arrival time with respective to reservoir parameter *m* is computed with Eq. A.4 as

$$
\frac{\partial t}{\partial m} = \frac{\dfrac{\partial \tau}{\partial m}}{\dfrac{\partial f_w}{\partial S_w}} = -\frac{\dfrac{\Delta \tau}{k(\mathbf{x})}}{\dfrac{df_w}{dS_w}} \tag{A.8}
$$

The time of flight sensitivity in Eq. A.4 plays a critical part of the analytical formulation of GTT of WWCT sensitivity.

APPENDIX B

FAST MARCHING METHOD

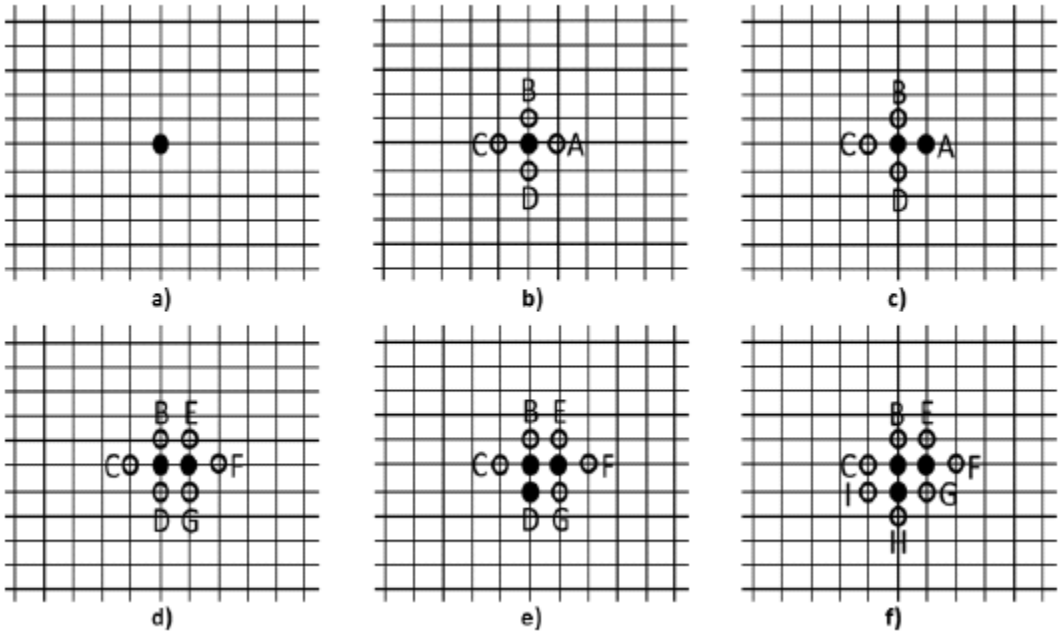

Figure B.1 Schematic description of the fast marching method showing the propagation of pressure waves in an orthogonal mesh grid

Figure B.1 shows an illustration of the Fast Marching Method, where the well location is first labeled as 'accepted' points (τ=0). Their adjacent nodes are labeled as 'neighbor' points and the rest nodes are called 'far-away' points. Now to calculate the arrival time at each point, the following procedure is applied:

1. Start from the 'accepted' points,
2. Calculate the arrival time of their 'neighbor' points (A, B, C, D, etc.) using the finite difference approximation

3. Pick the minimum arrival time in the current ‘neighbor’ points,
    - Label it as ‘accepted’ (e.g., Point A in B-1b)
    - Add its neighbors that are in ‘far-away’ as ‘neighbors’, (e.g., Points E, F & G in B-1d)
4. Repeat steps 2 and 3 until all the points in the domain are labeled as ‘accepted’.

APPENDIX C

DYNAMIC MEASURE THROUGH DRAINAGE VOLUME CALCULATION WITH FAST MARCHING METHOD

In chapter II, we showed how we formulate the dynamic measure for green field. The proposed dynamic measure is composed of static and dynamic properties which are permeability, pore volume and diffusive time of flight (DTOF) and it is expressed as follows,

$$Dynamic\ Measure(DM\_FMM) = (DTOF_{RN} \cdot PoreVolume_{RN} \cdot k_{RN}) \qquad (3.9)$$

Here, the term, DTOF, is the measure of how fast the pressure front from source or sink spreads out in the reservoir. In other words, it can be a way of calculating the drainage volume from the well. As we discussed in chapter II, we can obtain the pressure front propagation arrival time at each grid by applying the fast marching method. When the pressure front arrives at that grid, it indicates that this grid is starting to be drained. The mesh grids which have smaller values of arrival time than the considered time have already been drained. Therefore, the drainage volume at any time can easily be estimated by summing up the pore volumes of the mesh grids within that time contour. So, if we know the physical propagation time from the well, then we can calculate the drainage volume of the well at the considered time. It is explained how the physical propagation time is obtained from DTOF value in Xie et al. (2012)'s work.

The following pictures shows you that how we calculate drainage volume (DV) from the two wells drilled at different time.

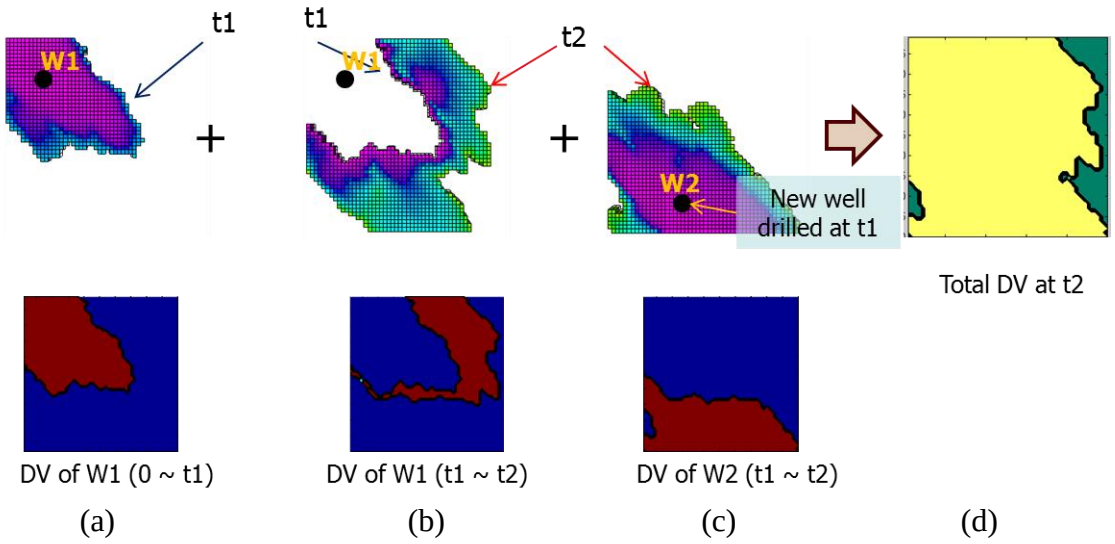

Figure C.1 Calculation of drainage volume from two wells

Suppose well 1 (W1 in the figure C.1) was drilled initially and we are looking for the optimal well location for the new well 2 (W2 in the figure C.2) at time, t1. Since well 1 has been producing until the time t1, well 1 has drainage volume from the well 1 itself to the contour of physical propagation time of t1 (figure C.1 (a)). After the time t1, we need to calculate drainage volume of two wells. During the time period from t1 to t2 (the considered time), the propagation of well 1 starts from the contour of well 1 at the time of t1 and the propagation of the well 2 starts from well 2 itself. The cells in the reservoir will have two propagation time values from two wells. At this time, we should compare the incremental propagation time (which is t2 – t1) from the contour of well 1 from t1,

with the incremental propagation time from the well 2. Figure C.1 (b) and (c) shows the drainage volume for each well during the time span, t1 to t2. For overlapped regions, if a cell has the smaller incremental propagation time from well 1, then the cell is thought be drained from the well 1 first and is included the drainage volume of well 1.

Since our goal is to find a well location to produce maximum production, we will choose the possible well location of well 2 that gives us the biggest total drainage volume. If we have more drainage volume from the well 1 and well 2, we expect to have more production. In this sense, dynamic measure for green filed using fast marching method can be expressed as,

$$Dynamic\ Measure\left(DM\_FMM\_DV\right)=\left(DV_{RN}\cdot k_{RN}\right) \tag{C.1}$$

Here, dynamic term is drainage volume which incorporates pore volume in it and static properties is permeability. Note that the drainage volume is the total drainage volume of existing and new wells. Fig. C.2 shows comparison of dynamic measure with drainage volume calculation and the result of commercial software. We obtained good match with the actual simulation results.

However, for this dynamic measure, we have to calculate total drainage volume exhaustively for the possible well location. Because the computational efforts of fast marching method is much less compared to commercial simulator, it doesn't take lots of computational time. But, it is true that we need to calculate according to the number of possible well locations whereas our proposed dynamic measure in chapter II needs a

single calculation. But, this approach may be a hint for how to deal with optimization problems of multiple wells drilled at different times with fast marching method.

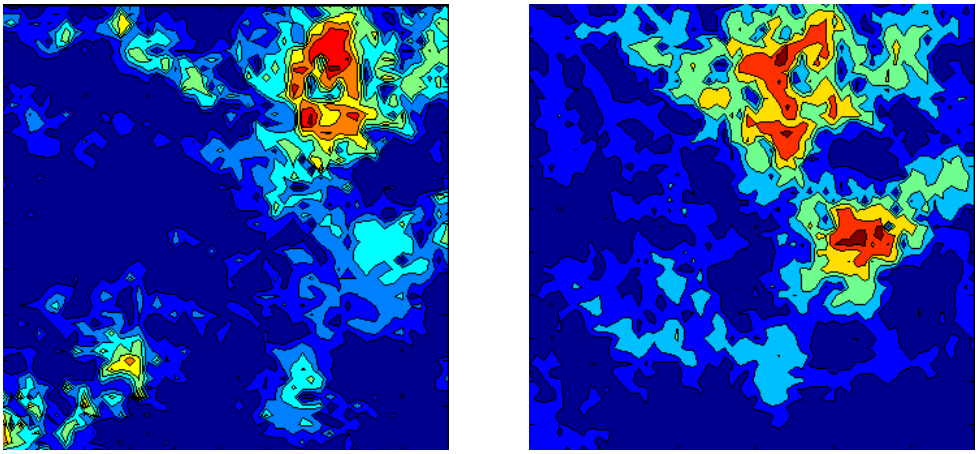

(a) (b)

Fig. C.2 (a) Dynamic measure with DV calculation (b) Exhaustive calculation results from commercial simulator